Microelectronics Reliability 55 (2015) 293–307

Contents lists available at ScienceDirect

Microelectronics Reliability

journal homepage: www.elsevier.com/locate/microrel

Introductory Invited Paper

A unified look at the use of successive differentiation and integration in MOSFET model parameter extraction

Francisco J. García-Sánchez [a,*], Adelmo Ortiz-Conde [a], Juan Muci [a], Andrea Sucre-González [a], Juin J. Liou [b,c]

[a] Solid State Electronics Laboratory, Simón Bolívar University, Caracas 1080A, Venezuela
[b] Department of Electrical and Computer Engineering, University of Central Florida, Orlando, FL 32816, USA
[c] Department of Information Science and Electronic Engineering, Zhejiang University, Hangzhou 310027, China

ARTICLE INFO

Article history:
Received 15 November 2014
Accepted 17 November 2014
Available online 6 December 2014

Keywords:
MOSFET model parameter extraction
Successive differentiation
Successive integration
Threshold voltage
Minimalist MOSFET model

ABSTRACT

This article provides a unified look at MOSFET model parameter extraction methods that rely on the application of successive differential and integral operators, their ratios, and various other combinations thereof. Some of the most representative extraction procedures are assessed by comparatively examining their ability to extract basic model parameters from synthetic MOSFET transfer characteristics, generated by an ad hoc minimalist four-parameter model. The model used, comprised of a single polylogarithm function of gate voltage, approximately describes in a very concise manner the essential features of MOSFET drain current continuously from depletion to strong inversion. The exponential-like low voltage and monomial-like high voltage asymptotes of this simple model are conveniently used to analyze and compare the different extraction schemes that are founded on successive differentiation or integration. In addition to providing a combined view useful for comparative methodological appraisal, the present unified analysis facilitates visualizing and exploring other potentially promising extraction strategies beyond the straightforward use of successive differential and integral operators and their ratios. We include examples of parameter extraction from measured transfer characteristics of real experimental MOSFETs to comparatively illustrate the actual numerical implementation of typical successive differential and integral operator-based procedures.

1. Introduction

Efficient parameter extraction strategies are essential for effective use of MOSFET compact models in circuit design and simulation. Model parameter extraction schemes and procedures are also indispensable tools to support device design assessment, technology reliability evaluation, and production yield analysis. Over the years numerous schemes have been devised to permit, facilitate and expedite the extraction of MOSFET model parameters [1–11]. Some schemes directly extract the parameters from the measured current–voltage characteristics or from their numerically calculated first and higher order derivatives, while others make use of certain auxiliary functions that typically involve calculating certain ratios of the drain current and its derivatives. Although differentiation of MOSFETs' measured current–voltage characteristics is crucial for describing and analyzing device operation, performing successive (repeated) numerical differentiation operations directly on raw and usually noisy experimental drain current data might not always be the most desirable practice, since any noise present would be repeatedly magnified by differentiation. Thus, some sort of noise-canceling or mitigating data-smoothing processing means is frequently included into any differentiation-based model extraction procedure [12–14].

Because numerical integration inherently diminishes measurement noise instead of enlarging it as differentiation does, our group has been advocating for a while the use of integration-based auxiliary functions, as an advantageous alternative to the traditionally used differentiation-based model parameter extraction techniques [15–23]. Numerical integration has already proved to be a useful tool for model parameter extraction in various situations where noisy experimental data is present [24], as well as for other kinds of analytical tasks, such as assessing harmonic distortion, for example [25–27].

The motivation of this article is to offer a unified systematic overview of successive differential and integral operators used in MOSFET model parameter extraction procedures. This approach allows a methodical classification and analysis of existing

* Corresponding author.

http://dx.doi.org/10.1016/j.microrel.2014.11.013
0026-2714/

procedures that are based on both types of these operators, and on combinations of two or more of them. The unified vision offered here greatly facilitates revealing the analogous procedural extraction features, and helps identify other possible successive operator combinations that could turn out to be useful for constructing new MOSFET model parameter extraction procedures. This type of joint look at differentiation and integration is a useful means to comparatively analyze model parameter extraction procedures in general, as has been done recently to compare existing methods to extract the series resistance of solar cells [28].

This article's structure is as follows: In Section 2 we introduce a novel minimalist general model of MOSFET transfer characteristics. This model consists of a simple equation, based on a polylogarithm function, which is continuously valid from sub-threshold to strong conduction. Its main purpose is to act as a simple convenient tool to analytically generate the synthetic transfer characteristics used to illustrate and compare all the different extraction procedures that will be analyzed throughout this article. The adequacy of this new abridged model as a sufficient general description of transfer characteristics will be verified in a particular example to model the transfer characteristics of experimental poly-Si Nano-Wire MOSFETs. Original measured data and the resulting playback using this model are later shown in Fig. 8 of Section 8.

A short-hand notation to represent successive operators in a concise manner will be briefly presented in Section 3 to be used throughout the text for brevity's sake. In Section 4 we introduce the unified expression to generically represent any successive operator in the abbreviated notation.

In Section 5 we describe the use of zero, first and higher order operators, and discuss some archetypal single operator-based extraction procedures. We then present in Section 6 some of the most commonly used procedures that are based on ratios of successive differential and integral operators. We describe the reasons behind the idea of the generic successive operator ratio, and discuss some important illustrative examples, such as the Transconductance-to-Current Ratio (TCR), the H_1 function, and the Y function.

The new concept of using successive operator triplets for parameter extraction is introduced in Section 7. The possible use of such triplets is illustrated by applying some of them to an extraction application. Additionally, in this section we discuss how to best choose an operator triplet's successive order from a qualitative point of view.

Section 8 presents a practical application example of parameter extraction from experimental Poly-Si Nano-Wire MOSFETs transfer characteristics measured in the linear and saturation operation regions. The effect of real measurement noise on the extraction procedure and on the ensuing accuracy of the extracted parameters is illustrated using the measured data. Special focus is placed, within the framework of this unified view, on the comparison of the advantages and disadvantages of applying differential operator-based procedures versus applying their equivalent integration-based counterparts.

Section 9 presents the various types of successive operator methods classified according to their utility to extract particular model parameters. Finally, Section 10 offers an overall consolidated picture and some general concluding remarks and considerations. An Appendix A is also included to provide some features of the polylogarithm function, relevant to the use of the presently proposed model.

2. A simple empiric MOSFET transfer characteristics model

In order to be able to compare the various differential and integral operator-based MOSFET model parameter extraction concepts and techniques, we need to apply each extraction procedure to a set of characteristics synthetically generated by the same MOSFET model. The model to be used for this purpose must be simple in mathematical terms and as minimalist as possible in the number of parameters it contains.

There have been several attempts and proposals for simple transregional single-equation MOSFET models, with only a few intuitive parameters, that cover sub-threshold as well as above-threshold regions [29–31]. The specific model that we use here to generate, test and compare extraction procedures is not crucial, as long as it is generic enough to satisfactorily describe the most essential physical features represented by the model parameters that we wish to extract. In that respect, and bearing in mind that accurate threshold voltage determination is one of the most vital aspects of parameter extraction, the model needs to describe the MOSFET's transfer characteristics by a simple continuous mathematical function that can be repeatedly differentiated within the threshold transition region. On the other hand, these attributes should be possible without having to resort to any of the many existing mathematically complicated MOSFET models. With these premises in mind, we present in the following paragraphs a simple empiric model that is able to satisfactorily describe the essential quasi-static features of a generic MOSFET's transfer characteristics, as a practical way of comparing the several parameter extraction procedures that will be analyzed here.

2.1. A novel transregional polylogarithmic model equation

We propose here a novel empiric transregional (continuous) mathematical description capable of approximately modeling the most relevant quasi-static features of the transfer characteristics of a broad variety of inversion mode MOSFETs, including conventional mono-crystalline, amorphous, poly-crystalline and organic devices [32], and perhaps some unconventional MOSFETs as well.

The derivation of the present model is outside the purpose of this article. Suffice to say that it is an empiric formulation phenomenologically motivated by the gate voltage dependence of the total carrier density in the MOSFET's channel. It is mathematically described by a function [33] (see Appendix A) inspired by the polylogarithm representation of the Fermi–Dirac Integral (*FDI*) [34,35]. Thus, and without further justification, we propose expressing the model using a polylogarithm function of the gate voltage, V_G, as a generic "first level" quasi-static description of a MOSFET's transfer characteristics:

$$I_D(V_G) = -K\,\mathrm{Li}_m\left(-e^{\frac{V_G-V_T}{n\,v_{th}}}\right), \tag{1}$$

where $\mathrm{Li}_m(\cdot)$ stands for the polylogarithm [33] of order m and argument $-\exp(\cdot)$ [36]. We adopt this simple Eq. (1) as the core structure of the proposed model. It contains only the essential quasi-static features, which are represented by four basic parameters: (i) a generic specific current parameter K, with global units of Amperes, which reflects physical and geometrical characteristics and depends on the magnitude of the drain voltage, V_D, and could eventually include an additional dependency on V_G; (ii) a dimensionless sub-threshold factor $n = SS\ln(10)/v_{th}$, where SS is the so-called *S*ub-threshold *S*lope or *S*wing, with units of Volts/decade of drain current; (iii) an explicit threshold voltage V_T (or V_{on} as in other models) with units of Volts; and (iv) a dimensionless above-threshold monomial order exponent m, representing the effect of mobility degradation or enhancement, and possibly also including the effect of significant parasitic source and drain (R_{SD}) series resistance. Thus in general $m \neq 1$, unless both of these effects were to be taken care of externally to an idealized intrinsic MOSFET core model with an m equal (or very close) to unity.

2.2. Comparison with other models

The presently proposed model, as defined by the polylogarithm function in (1), mathematically resembles the form of the well known EKV model, where the drain current is empirically described by a function of the type $(\ln(1+e^{x}))^2$ [31]. The form of the EKV model is very similar to the present model, since its function is nothing more than the square of a polylogarithm of order $m = 1$, as pointed out below in (2). Furthermore, the proposed model defined by (1) also bears a general resemblance to another well known model: the ACM model, which is based on a more physically meaningful Lambert W function-type equation [31], instead of the more empirical polylogarithm form of the present and EKV models.

The present transregional model is continuous and may be continuously and repeatedly differentiated throughout depletion, weak, moderate, and strong inversion regions of operation. It is also analytically and numerically manageable, given that major symbolic and numeric mathematical software packages, such as *Mathematica* and *Maple* and others, already have efficient built-in algorithms in their libraries to calculate the polylogarithm function. Moreover, it is foreseeable that most circuit simulation programs, that have not yet done so, will soon seamlessly incorporate this and other useful mathematical functions, such as the important Lambert$W$ function [37,38], that are indispensable for proper electron device modeling and simulation.

Unlike most other continuous transregional MOSFET models, the present abridged description (1) offers the advantage of explicitly incorporating the threshold voltage, V_T, among its four basic parameters. Such unequivocal presence of V_T in the model equation constitutes a necessary characteristic for an unambiguous validation of any threshold voltage extraction procedure. Satisfactory extraction of the above mentioned basic four parameters constitutes the basis for judging the adequacy of any prospective auxiliary function for parameter extraction purposes.

Idealized MOSFET transfer characteristics – with perfectly linear current above V_T due to the absence of any V_G-dependence of the mobility or significant R_{SD} – can be modeled with (1) by letting the polylogarithm's order be unity ($m = 1$). In such case this model (1) reduces to an elementary expression of the form (see (A2.9) in Appendix A):

$$I_D(V_G)|_{m=1} = K \ln\left(e^{\frac{V_G - V_T}{n\, v_{th}}} + 1\right). \tag{2}$$

At gate voltages below V_T the above Eq. (2) becomes an exponential function of V_G, and at gate voltages well above V_T it becomes a linear function of V_G. In contrast to (2), the use of an arbitrary order polylogarithm in the proposed model (1) allows accounting for the presence of nonlinear drain current behavior above V_T, approximately described by a power function (a monomial function of order $m \neq 1$).

2.3. Above- and below-threshold asymptotes

Let us now take a closer look at the low and high V_G asymptotes to verify that (1) is indeed adequate to describe in general the expected below- and above-threshold transfer characteristics of MOSFETs. At high gate voltages the asymptote of (1) is a monomial function of order m given by [39]:

$$I_D(V_G >> V_T) \Rightarrow \frac{K}{\Gamma(m+1)(n\, v_{th})^m}(V_G - V_T)^m \quad , \tag{3}$$

where Γ is the Gamma function [40].

Therefore, the use of this model (1) implies the assumption that it is possible to approximately describe the above-V_T drain current's strong conduction non-linear behavior by a single monomial-type function of V_G of order $m \neq 1$. This assumption is particularly well suited for amorphous, poly-crystalline and organic MOSFETs, whose above-V_T drain currents are commonly modeled by a fractional order power function of V_G (an mth order monomial on V_G with a fractional value of m) [10,32,41–44]. Although monomial-type descriptions of strong inversion, such as (3), have been traditionally reserved for non-crystalline MOSFETs, we propose to extend such monomial portrayal to other types of FETs, as a useful and sufficiently adequate first level generic approximation of the, usually non-linear, above-V_T behavior observed in general in most inversion mode MOSFETs. Note that specific values of $m = 1$ and $m = 2$ in (3) respectively correspond to the classical "first level" models of the above-V_T transfer characteristics in the linear (low V_D) and to the saturation (high V_D) regions of intuitively idealized conventional bulk-type mono-crystalline inversion mode MOSFETs.

A monomial description of the above-V_T drain current at low V_D could be interpreted assuming that any non-unitary value of m includes the portrayal of a gate voltage dependence of the mobility, and could also represent the degradation effect caused by parasitic source and drain series resistance (R_{SD}), whenever it is decided not to treat it as an extrinsic effect. To spell out this kind of interpretation of m, we may split this exponent into a sum of two parts: $m = 1 + \beta$, where β is meant to account for the gate voltage dependence of the mobility (and the effect of R_{SD} if that where the case). Thus, at low V_D, values of m between 0 and 1 (that is $-1 < \beta < 0$) are indicative of mobility (and/or R_{SD}) degradation; whereas values of $m > 1$ (that is $\beta > 0$) are indicative of the manifestation of mobility enhancement, a phenomenon frequently observed in non-crystalline devices [45]. A similar interpretation could be applied to high values of V_D above saturation, except that in that case $m = 2 + \beta_{sat}$.

The below-V_T drain current of conventional inversion mode MOSFETs is usually dominated by diffusive transport, represented by exponential behavior that is adequately described by the low voltage asymptote of the simple model (1) given by:

$$I_D(V_G << V_T) \Rightarrow K\, e^{\frac{V_G - V_T}{n\, v_{th}}}, \tag{4}$$

This below-V_T drain current Eq. (4) is independent of m and for most MOSFETs increases exponentially with gate bias, V_G, according to a sub-threshold characteristic parameter n, until it approaches the threshold voltage V_T in the transition region, where its behavior changes from exponential-like to monomial-like. Parameter n defines the *S*ub-threshold inverse *S*lope or *S*wing by the relation: $SS = \ln(10) n v_{th}$, which is usually expressed in units of mV/decade of drain current. In real inversion mode MOSFETs this parameter usually is $n > 1$, corresponding to $SS \geqslant 60$ mV/dec at $T \approx 300$ K.

Fig. 1 presents typical synthetic transfer characteristics in linear and semi-logarithmic scales, as simulated with the presently proposed simple model defined by (1), using parameter values indicated within the figure. The drain current curves illustrated in Fig. 1 exhibit the expected exponential-type sub-threshold behavior and the above-V_T super-linear monomial type behavior that correspond to the given values of n and m.

3. Shorthand notation for successive differential or integral operators

The intended meaning attributed here to successive differential or integral operations is the action of computing a derivative or an integral of the original function, successively repeated a certain number of times with respect to a specified single variable. In the present context of parameter extraction procedures, this means that the actual numerical operations of either differentiation or integration will be repeatedly performed, a certain number

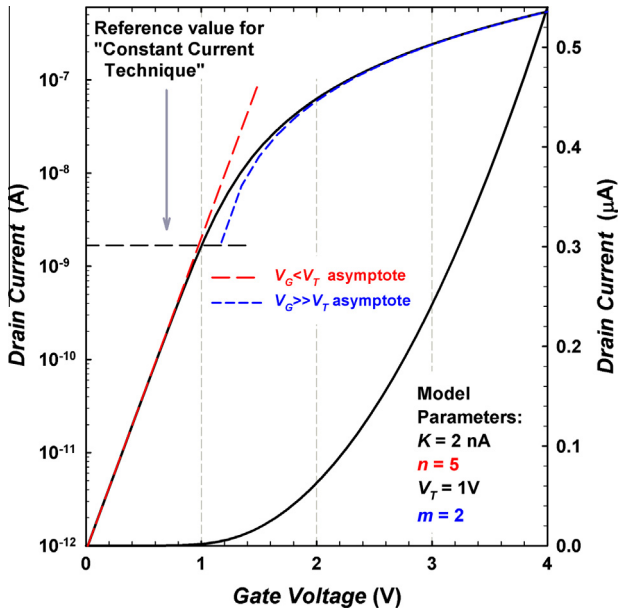

Fig. 1. Illustrative example of generic synthetic MOSFET transfer characteristics as generated with the proposed abridged model of (1) (solid black lines). Also shown in semi-logarithmic scale with broken lines are the above threshold ($V_G \gg 1$ V) (short dash blue line) and below threshold ($V_G < 1$ V) (Long dash red line) asymptotes of (1), corresponding to (3) and (4) respectively. A horizontal broken line is also shown to indicate the critical value of drain current that would define threshold according to a constant current criterion (9). (For interpretation of the references to colour in this figure legend, the reader is referred to the web version of this article.)

of times indicated by the operator order's absolute value $|\alpha|$, on a MOSFET's drain current numerical data, that has been measured by varying the applied gate voltage while keeping the drain voltage constant at a certain value.

For brevity's sake, a superscript-style shorthand notation will be used throughout the text to indistinctly represent successive (successively repeated) differential or integral operations with respect to gate voltage. This abbreviated operator notation is as follows:

$$I_D^{(\alpha)}(V_G) = \begin{cases} d^{\alpha} I_D(V_G)/dV_G^{\alpha} & \text{when } \alpha \geq 1 \\ I_D(V_G) & \text{when } \alpha = 0 \\ \int_0^{V_G} \int_0^{V_G} \cdots \int_0^{V_G} I_D(v)\, dv_{-1} dv_{-2} \ldots dv_{\alpha} & \text{when } \alpha \leq -1 \end{cases}, \tag{5}$$

where the operator's order (α) can be any real integer number. A value $\alpha = 0$ represents the function itself (the device's measured original I_D). The sign of α defines the type of operation that is to be performed: positive values of α denote differentiation, whereas negative values of α denote integration. In the case of integration, we will assume here, for simplicity's sake and without any loss of generality, that the magnitude of the function I_D is zero (or insignificantly small) at the lower limit of integration, so that the definite integrals in (5) may be conveniently subsumed as indefinite integrals. When in actual practice the magnitude of the function I_D cannot be assumed to be zero, because of the presence of significant leakage current, that value must be used as the lower limit of integration and definite integrals must be used for actual computation.

4. Application of successive operators to the present model

Assuming that the MOSFET's transfer characteristics may be adequately modeled by (1), the application of any successive operator of order α to (1), be it differential ($\alpha > 0$) or integral ($\alpha < 0$), always yields an expression that may be written in the following general form:

$$I_D^{(\alpha)} = -K(n\, v_{th})^{-\alpha} \mathrm{Li}_{m-\alpha}\left(-e^{\frac{V_G - V_T}{n\, v_{th}}}\right). \tag{6}$$

Thus, any successive operator of order α when applied to the current, as modeled by a polylogarithmic function of order m described in (1), is given by the expression (6) which also contains a polylogarithm but in this case of order $(m-\alpha)$. This simply means that performing a successive operation of order α ($\alpha > 0$ for differential or $\alpha < 0$ for integral) on the polylogarithm-type current expression decreases (when $\alpha > 0$) or increases (when $\alpha < 0$) its order m by an amount equal to $|\alpha|$. Notice that the zero order ($\alpha = 0$) operation, $I_D^{(0)}$, translates (6) into the original function itself, given by (1).

Analyzing the asymptotic behavior of (6), considering (3), we observe that well above V_T the function (7) tends asymptotically to a monomial function of gate voltage of order $(m-\alpha)$:

$$I_D^{(\alpha)} \Rightarrow \frac{K(n\, v_{th})^{-m}}{\Gamma(m-\alpha+1)}(V_G - V_T)^{m-\alpha}, \quad \text{for } V_G >> V_T \tag{7}$$

Likewise, considering (4) we observe that well below V_T (6) tends asymptotically to an exponential function of gate voltage, which is independent of m as expected:

$$I_D^{(\alpha)} \Rightarrow K(n\, v_{th})^{-\alpha}\, e^{\frac{V_G - V_T}{n\, v_{th}}}, \text{ for } V_G << V_T. \tag{8}$$

Any member of the family of successive operators defined by (6) may be used, either singly or combined in groups, to construct clever numerical calculation procedures which when applied to the MOSFET's measured current–voltage characteristics facilitate the extraction of the device's model parameters. In what follows we will analyze several of the most common and presently used extraction procedures, and will later discuss some other possible schemes.

5. Extraction procedures based on a single operator

5.1. The zero order operator

Strictly speaking the drain current is the zero order ($\alpha = 0$) operator of itself ($I_D^{(0)}$). Thus, the simplest single operator threshold voltage extraction procedure is the well known and Industry-favored "constant current" method [46–50]. Extraction of the value of the threshold voltage parameter, V_T, using this definition involves the trivial chore of looking up the value of gate voltage that corresponds to a certain pre-defined value of drain current in the measured transfer characteristics data. Because of its simplicity and its fast implementation this constant current method is usually preferred in industrial testing settings.

Although the value of constant drain current to use is arbitrary, its choice is not directly trivial. Traditionally this value has been independently decided in-house by each user on the basis of some more or less arbitrary particular criterion. To avoid such ambiguity there have been proposals to generalized the choice based on some sort of standard current density criterion [47,49]. Here we suggest to use a single criterion to establish a normalized universal constant current value by letting $V_G = V_T$ in (1), as illustrated by the horizontal dashed line in Fig. 1. Accordingly, this normalized reference value will be given by the following defining equation (see (A4.2) and (A4.3) in Appendix A):

$$\frac{I_D(V_G = V_T)}{K} = -\mathrm{Li}_m(-1) = \begin{cases} \ln(2), & \text{at } m = 1 \\ -\left(2^{1-m} - 1\right)\zeta(m), & \text{for } m > 1 \end{cases}, \tag{9}$$

where ζ is the Riemann Zeta function [51]. Therefore the normalized values that correspond to the condition $V_G = V_T$, given by (9),

have a slight dependence on the monomial order m, varying from 0.69 at $m = 1$, to 0.82 at $m = 2$, to 0.90 at $m = 3$.

5.2. First order operators

Perhaps the most common way to extract the threshold voltage parameter of a MOSFET is the classical method based on the "linear extrapolation" of the strong inversion (above-V_T) drain current to zero (gate voltage intercept). Performing such extrapolation entails calculating the $\alpha = 1$ order operator, that is, the first order derivative $I_D^{(1)}$ (slope) of the transfer characteristics. This method is based on the assumption that the ideal strong inversion (above-V_T) drain current is a linear function ($m = 1$) of V_G. This assumption is frequently implicitly taken for granted for V_T extraction purposes, in spite of the fact that such ideal linearity is theoretically impossible [4].

The drain current measured in strong inversion of real monocrystalline MOSFETs usually exhibits sub-linear ($0 < m < 1$) behavior due to the combined effects of mobility degradation and parasitic source and drain resistance, as well as several other secondary effects. Nonetheless, is not uncommon to see the use of this linear extrapolation method for V_T extraction, even when the above-V_T transfer characteristics appear to be clearly non-linear. To do so, the method is forced upon the non-linear characteristics by extrapolating a line tangent to the point where the transfer function presents its maximum slope (the inflexion point of $I_D^{(0)}$ or maximum of the transconductance $I_D^{(1)}$). This maximum of the transconductance exists if and only if $m < 1$ in (1), that is, as long as there is mobility degradation or parasitic series resistance present, in which case the maximum is uniquely defined by the location of $I_D^{(2)} = 0$ (the zero crossing of the second derivative). Since the location of this maximum is strongly dependent on mobility and parasitic resistance effects, the V_T so extracted by extrapolation is highly questionable value. On the other hand, a maximum of the transconductance might not even exist in certain cases, especially when there is mobility enhancement ($m > 1$) instead of degradation.

A general word of caution is called for whenever regional extrapolation-based extraction procedures are used. Any parameter value extracted in this manner should always be understood only as an extended description of the physical phenomenon it represents. It should be remembered that the phenomenological behavior description that is assumed to be valid within the region where the extrapolation originates from, should not be extended by the extraction procedure to a different region where it is not strictly valid. Therefore, in general it is preferable, whenever possible, to extract a phenomenological transition parameter such as V_T from the function's transition region itself, rather than by extrapolating a behavioral description belonging to a different operation region.

It is also possible to use the $\alpha = -1$ order operator in parameter extraction, that is, the first order integral $I_D^{(-1)}$ (area) of the transfer characteristics. To the best of our knowledge, the use of the integral $I_D^{(-1)}$ of the current was first proposed by Araujo and Sánchez [52] for extracting series resistance in solar cell models, and it was later used for threshold voltage extraction in MOSFET models [24,53].

5.3. Higher order operators

Higher order successive operators are also very useful for model parameter extraction purposes. Repeated differentiation of the drain current is the most emblematic example for extracting the value of the threshold voltage, V_T [54]. It belongs to the class of transitional techniques used to extract V_T instead of the classical linear extrapolation procedure. In its simplest form it entails finding the location of the maximum of some high order ($\alpha > 1$) derivative $I_D^{(\alpha)}$ of the MOSFET's transfer characteristics.

Considering an ideal MOSFET's transfer characteristics that are hypothetically described in strong inversion by a straight line (a monomial function of gate voltage with $m = 1$), the second order ($\alpha = 2$) differential operator $I_D^{(2)}$ should exhibit a maximum located on the V_G axis precisely at V_T. This is the basis of the extraction procedure commonly known as "maximum of the second derivative" or "maximum of the transconductance's slope" technique [10,55] which is the most representative example of successive differential operator usage for parameter extraction purposes. The extraction of V_T only requires numerically locating the value of V_G where the third order ($\alpha = 3$) differential operator changes sign, i.e., $I_D^{(3)}$ ($V_G = V_T$) = 0, the location where $I_D^{(3)}$ crosses the V_G axis.

The threshold voltage extracted by this technique can be rightfully identified as a "transitional" kind of V_T value, because the extraction occurs from within the very region where the actual transition from sub- to supra-threshold behaviors takes place. The value of V_T so extracted has the added advantage of being less dependent upon other phenomena, since the current in this region is relatively more immune to other secondary effects such as mobility degradation and parasitic source and drain resistances.

Regrettably the "maximum of the second derivative" technique is often misused. The procedure is sometimes applied without valid justification to extract the V_T of FETs that do not exhibit unmistakable linear currents in strong inversion. We will attempt to illustrate this misconceived usage by comparing two normalized hypothetical transfer characteristics with equal values of V_T but dissimilar above V_T conduction mechanisms: one ideally linear ($m = 1$) and the other non-linear ($m = 1.5$). The non-linear behavior may be caused by different phenomena, for instance, by some kind of V_G-dependent mobility enhancement, as frequently observed in non-crystalline MOSFETs.

Fig. 2 presents the first three successive derivatives ($\alpha = 1$, 2, and 3) of both types of hypothetical transfer characteristics. As the figure indicates, the third order ($\alpha = 3$) differential operator $I_D^{(3)}$ correctly crosses the V_G axis exactly at V_T in the case of the linear above-V_T characteristics ($m = 1$), but not so in the case of the non-linear ($m = 1.5$) behavior. The reason is easily visualized using the present abridged model (1) by noticing in (6) that any successive derivative $I_D^{(\alpha)}$, when evaluated at threshold, $V_G = V_T$, contains a polylogarithm of order (m–α) and argument ($-e^0 = -1$), as indicated below:

$$I_D^{(\alpha)}(V_G)\Big|_{V_G=V_T} = -K(n\,v_{th})^{-\alpha}\,\mathrm{Li}_{m-\alpha}(-1). \tag{10}$$

In order for (10) to become nontrivially zero it is necessary that the polylogarithm in (10) be equal to zero, i.e. $\mathrm{Li}_{m-\alpha}(-1) = 0$. Now, the only polylogarithm that becomes zero at a value of its argument equal to -1 is the polylogarithm of order equal to -2 (see (A2.2) and (A4.1) in Appendix A). Therefore, if we let $m-\alpha = -2$ in (10) then $\mathrm{Li}_{-2}(-1) = 0$.

$$I_D^{(\alpha)}(V_G)\Big|_{\alpha=m+2,\ V_G=V_T} = -K(n\,v_{th})^{-m-2}\,\mathrm{Li}_{-2}(-1) = 0. \tag{11}$$

Solving for the operator order α we reach the following important conclusion:

"For any successive differential ($\alpha > 0$) operator $I_D^{(\alpha)}$ of the transfer characteristics to become zero exactly at threshold ($V_G = V_T$) its order α must be two orders higher than the order m of the monomial function that describes its above-V_T transfer characteristics, that is $\alpha = m + 2$."

Or alternatively stated:

"For any successive differential ($\alpha > 0$) operator $I_D^{(\alpha)}$ of the transfer characteristics to exhibit a maximum precisely at

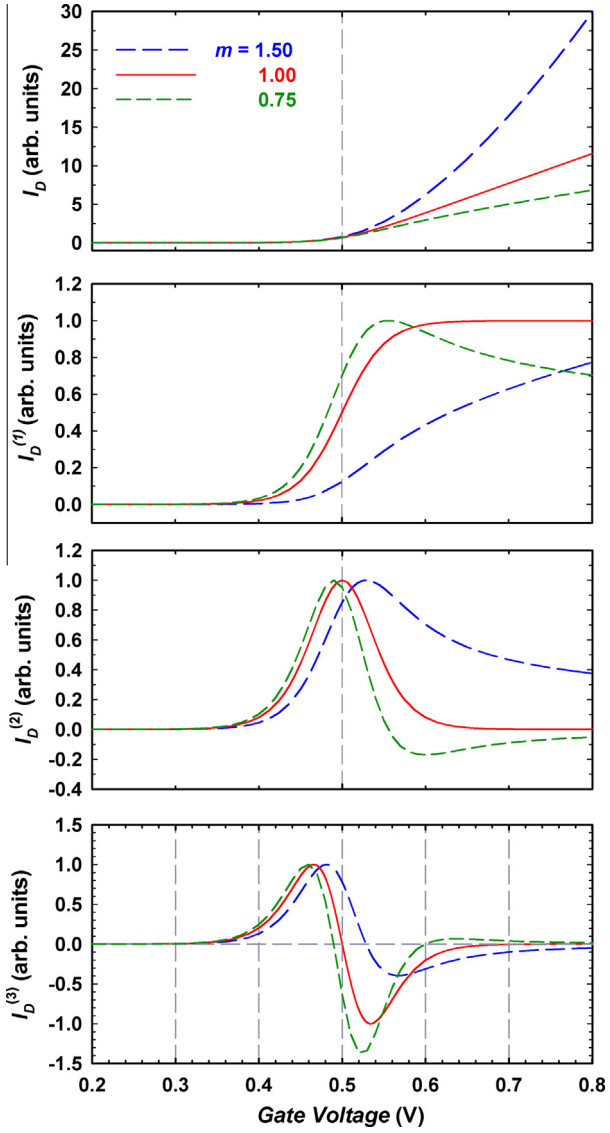

Fig. 2. Hypothetical synthetic transfer characteristics, and their first three successive derivatives ($\alpha = 1, 2, 3$), calculated using (6) with the same $n = 1$ and $V_T = 0.5$ V, for three different values of the monomial order parameter: $m = 0.75$ (short dash green line), $m = 1.0$ (continuous red line) and $m = 1.5$ (long dashed blue line). The slope ($I_D^{(2)}$) of the transconductance ($I_D^{(1)}$) has a maximum at $V_G = V_T$, if $I_D^{(3)} = 0$ at $V_G = V_T$, which only happens when the above-V_T current is a perfectly linear ($m = 1$) function, as illustrated. (For interpretation of the references to colour in this figure legend, the reader is referred to the web version of this article.)

threshold ($V_G = V_T$) its order α must be one order higher than the order m of the monomial function that describes its above-V_T transfer characteristics, that is $\alpha = m + 1$."

Consequently, according to this simple but universal rule, the second derivative of the transfer characteristics (commonly referred to as the transconductance slope) will exhibit a maximum precisely at threshold ($V_G = V_T$) if and only if the above-V_T transfer characteristics are sufficiently well represented by a linear function of V_G (a monomial of order $m = 1$).

Fig. 2 illustrates that when $m = 1$ the second order ($\alpha = m + 1 = 2$) differential operator (the second derivative $I_D^{(2)}$ of the current which corresponds to the transconductance's slope) has a maximum precisely at V_T. In other words, the third order ($\alpha = m + 2 = 3$) differential operator $I_D^{(3)}$ crosses the V_G axis precisely at threshold ($V_G = V_T$), meaning that $I_D^{(3)} = 0$ at $V_G = V_T$.

However, the same will not be the case when the above-V_T transfer characteristics are significantly nonlinear ($m \neq 1$). An illustrative example of this fact is presented also in Fig. 2, with above-V_T transfer characteristics described in this case by a monomial function of order $m = 1.5$. We observe that now the second order ($\alpha = 2$) differential operator $I_D^{(2)}$ (the second derivative or transconductance slope), does not have a maximum at V_T, and consequently the third order ($\alpha = 3$) differential operator $I_D^{(3)}$ does not cross the V_G axis at threshold, that is, $I_D^{(3)} \neq 0$ at $V_G = V_T$. In this case the polylogarithm's order in (10) is $\neq -2$, as needed to become zero at $V_G = V_T$. Instead it is now equal to $m - \alpha = 3/2 - 3 = -3/2$ which is $\neq -2$.

Using this value of $-3/2$ for the polylogarithm's order yields $-\mathrm{Li}_{-3/2}(-1) = 0.1187$, which is clearly $\neq 0$. In fact, the third order ($\alpha = 3$) differential operator $I_D^{(3)}$ crosses the V_G axis at a value of the polylogarithm's argument of ≈ -3.03, since $\mathrm{Li}_{-3/2}(-3.03) \approx 0$. Obviously, if we where to take this $I_D^{(3)} = 0$ (V_G axis intercept) point as representing the location of V_T in the case of these transfer characteristics which are non-lineal above-V_T and described by a monomial of order $m = 1.5$, we would be making an error of ≈ 29 mV at room temperature (with $n = 1$ and $v_{th} = 0.0259$V). Considering that in this example $V_T = 0.5$ V, the corresponding relative error would be $\approx 5.8\%$.

It immediately follows from the above discussion that for an $m = 2$, which would correspond to the classic first level theoretical descriptions of the above-V_T transfer characteristics in the saturation (high $V_D > V_{Dsat}$) operation region of an ideal bulk-type MOSFET, the threshold voltage saturation value V_{Tsat} should be extracted from the location of the maximum of its third derivative $I_D^{(3)}$, or what is the same, by numerically finding the V_G axis crossing of its fourth derivative, $I_D^{(4)} = 0$. In such case we ought to name this procedure as the "maximum of the third derivative" technique.

The foremost drawback for practical implementation of this technique in threshold voltage extraction procedures is its reliance on successive numerical differentiation of the measured transfer characteristics. Numerical calculation of successive derivatives is very sensitive to the presence of small perturbations (errors or noise) of the measured data. In principle it yields highly noisy and uncertain results that are generally inadequate for reliable parameter extraction purposes. Such data imprecision can be mitigated by the use of data smoothing steps [14], or by applying some kind of stable numerical differentiation technique [12]. A very powerful technique, based on Tikhonov's regularization theory, has been reported to allow stable threshold voltage extraction from the maximum of the measured current's second order derivative [13].

We are then lead to the conclusion that this method, based on the location of the maximum of some high order derivative, works well for extracting a transitional-type value of V_T, when the observed above-V_T strong conduction behavior may be sufficiently well represented by a monomial-like function of positive integer order. Conversely, whenever the device's above-V_T strong conduction behavior is better described by a positive fractional power function (a fractional order monomial-like function) this successive differentiation method will fail to extract a correct value of V_T. This is so because the fractional order prevents any successive derivative of the current ($I_D^{(\alpha)}$) from crossing the V_G axis precisely at the location of V_T.

As a final thought on this topic, we call attention to the important fact that, since the order of the monomial-like strong conduction current behavior is always positive ($m > 0$) for any kind of practical MOSFET, the order of the operator needed to observe a maximum must always be positive ($\alpha = m + 1 > 0$). The immediate consequence of this observation is that only differential, and not integral, successive operators may be used to implement parameter extraction procedures of this kind.

We have seen that single successive operators of order $\alpha \geqslant 0$ are by themselves helpful tools to use for parameter extraction

purposes. We have presented constant current, linear extrapolation, and transitional types of single operator extraction procedures as good examples. On the other hand, integral operators (of order $\alpha < 0$) are not in general very useful for parameter extraction purposes when used singly, except for very few particular applications, such as eliminating the effect of parasitic resistances from lumped parameter models [56,57]. However, both integral and differential successive operators turn out to be valuable instruments for MOSFET model parameter extraction when adequately combined in the form of ratios, products, triplets and various other assemblies. In the following sections we will discuss some of these combinations of successive operators in a unified way.

6. Extraction procedures based on ratios of successive operators

When developing any kind of procedure for model parameter extraction a fundamental aspiration is to have a method that is able to extract each model parameter in such a way that its extraction is as unaffected as possible by the rest of the model parameters. A common strategy is to cancel the effect of some parameters while extracting the values of others. This chore may sometimes be accomplished through the use of certain auxiliary functions composed of successive operator ratios. An early use of successive operator ratios can be found in a 1988 small signal evaluation of Schottky barriers and pn-junction *I–V* plots [58].

6.1. General expression of the successive operator ratio

In view of the generic operator definition given in (6) we can easily recognize that the ratio of any two successive operators of orders α and $\alpha - 1$ is given by:

$$\frac{I_D^{(\alpha)}}{I_D^{(\alpha-1)}} = \frac{1}{n\,v_{th}} \frac{\mathrm{Li}_{m-\alpha}\left(-e^{\frac{V_G-V_T}{n\,v_{th}}}\right)}{\mathrm{Li}_{m-(\alpha-1)}\left(-e^{\frac{V_G-V_T}{n\,v_{th}}}\right)}. \tag{12}$$

The most salient feature of any operator ratio is the ability to cancel out the effect of parameter K by virtue of the division. This is so as long as K itself is not a strong function of V_G so that it may be assumed to be a constant. Important as this cancelation might be, it is not the only beneficial consequence of the ratio described by (12). To visualize its possible usefulness, let us take a look at the asymptotes of this ratio. First of all, recalling (7) we see that well above V_T the inverse of (12) asymptotically tends to:

$$\frac{I_D^{(\alpha-1)}}{I_D^{(\alpha)}} \Rightarrow \frac{\Gamma(m-\alpha+1)}{\Gamma(m-\alpha+2)} \frac{(V_G-V_T)^{m-\alpha+1}}{(V_G-V_T)^{m-\alpha}} = \frac{1}{m-\alpha+1}(V_G-V_T)\,, \quad \text{for } V_G >> V_T\,, \tag{13}$$

which is a linear (order = 1) monomial function of V_G regardless of the monomial order of the original transfer characteristics $I_D{}^{(0)}$ in the strong inversion region ($V_G \gg V_T$). That means that above V_T the ratio is always a straight line. This is the most significant general property of the generic ratio (12). It has important consequences for parameter extraction, because it embodies a general procedure capable of "linearizing" any MOSFET's above-V_T transfer characteristics, regardless of the value of m. Therefore, its linearization capability is universal, working equally well on idealized hypothetical characteristics in the so-called linear ($m = 1$) and saturation regions ($m = 2$) regions, and on more physically real characteristics ($m \neq 1$) resulting from significant mobility enhancement ($m > 1$), mobility degradation ($m < 1$), or parasitic R_{SD} ($m < 1$).

On the other hand, for values of $V_G \ll V_T$ the polylogarithms in the numerator and denominator of the RHS of (12) cancel each other, since in that sub-V_T region the value of the polylogarithm [33] is independent of its order (see Appendix A). Therefore, and in accordance with (8), this generic ratio (12) below V_T tends asymptotically to:

$$\frac{I_D^{(\alpha)}}{I_D^{(\alpha-1)}} \Rightarrow \frac{(n\,v_{th})^{-\alpha}}{(n\,v_{th})^{-\alpha+1}} = \frac{1}{n\,v_{th}}\,, \quad \text{for } V_G << V_T, \tag{14}$$

which is independent of m.

We conclude that any auxiliary function based on the generic ratio of any two arbitrary but successive operators, as defined by (12), when applied to a MOSFET's transfer characteristics yields at low $V_G \ll V_T$ a constant value that is equal to the reciprocal of the sub-threshold parameter $nv_{th} = SS/\ln(10)$, as indicated in (14), where SS is the Sub-threshold Slope or Swing in units of Volts/decade of drain current. Moreover, the reciprocal of this same ratio defined by (12), when applied to the MOSFET's transfer characteristics always yields at high $V_G \gg V_T$ a linear function of V_G whose reciprocal slope defines the value of parameter m and its extrapolated V_G axis intercept is located at V_T, as indicated by (13).

We must insist again here that the V_T value obtained by extrapolating (13) to the V_G axis must be interpreted as a "regionally extrapolated" type of parameter, because it is obtained by extending the drain current behavior of the above-V_T region to the weak inversion transition region, where the actual drain current behavior is neither exponential nor monomial. Later on we will discuss a procedure, also based on successive operator ratios, that allows extracting a more phenomenologically correct "transition" type of V_T value from within the weak inversion transition region.

6.2. The Transconductance-to-Current Ratio

A specific example of a well known and commonly used auxiliary function is the Transconductance-to-Current Ratio (*TCR*) [50,59–67]. This function consists of the ratio of the two successive differential operators defined by setting $\alpha = 1$ in (12), as indicated below:

$$TCR \equiv \left.\frac{I_D^{(\alpha)}}{I_D^{(\alpha-1)}}\right|_{\alpha=1} \equiv \frac{I_D^{(1)}}{I_D^{(0)}} \equiv \frac{dI_D/dV_G}{I_D} = \frac{d\ln(I_D)}{dV_G}. \tag{15}$$

In writing (15) we have called upon a basic calculus identity to remind us that the *TCR* can be understood as the derivative of the natural logarithm of the current with respect to gate voltage. The *TCR* can be readily written in terms of the presently proposed abridged model, setting $\alpha = 1$ in (12) to yield the expression:

$$TCR = \frac{1}{n\,v_{th}} \frac{\mathrm{Li}_{m-1}\left(-e^{\frac{V_G-V_T}{n\,v_{th}}}\right)}{\mathrm{Li}_{m}\left(-e^{\frac{V_G-V_T}{n\,v_{th}}}\right)}. \tag{16}$$

The significance of (16) stems from its remarkable ability to extract useful information from every region of the MOSFET's transfer characteristics. In fact, it is easy to see that in addition of canceling the effect of K, setting $\alpha = 1$ in (13) and (14) the asymptotic behavior of *TCR* is:

$$\frac{1}{TCR} \equiv \frac{I_D^{(0)}}{I_D^{(1)}} \Rightarrow \frac{1}{m}\,(V_G-V_T)\,, \quad \text{for } V_G >> V_T\,. \tag{17}$$

$$TCR \equiv \frac{I_D^{(1)}}{I_D^{(0)}} \Rightarrow \frac{1}{n\,v_{th}}\,, \quad \text{for } V_G << V_T. \tag{18}$$

Up to this point we have only analyzed examples of parameter extraction procedures based on differential operators ($\alpha \geqslant 0$). Let us now look also into some extraction procedures examples that are based on integration ($\alpha < 0$) instead of differentiation.

6.3. The H_1 function

Although using the *TCR* procedure is a widespread practice in MOSFET parameter extraction, it is by no means the only successive operator ratio that is capable of achieving the same goal. In fact, a conceptually analogous but less well known successive operator ratio is the Integral-to-Current Ratio, or H_1 auxiliary function [16,19,22,23]. This H_1 function (its symbol is H because of historic reasons and should not be confused with a Hermite polynomial) was originally suggested as a means to extract the model parameters of *p-n* junction models at very low forward voltages [15]. The reciprocal of the H_1 auxiliary function can be quickly written using the presently proposed abridged model by setting $\alpha = 0$ in (12) to yield:

$$1/H_1 \equiv \left.\frac{I_D^{(\alpha)}}{I_D^{(\alpha-1)}}\right|_{\alpha=0} \equiv \frac{I_D^{(0)}}{I_D^{(-1)}} = \frac{1}{n\,v_{th}} \frac{\mathrm{Li}_m\left(-e^{\frac{V_G-V_T}{n\,v_{th}}}\right)}{\mathrm{Li}_{m+1}\left(-e^{\frac{V_G-V_T}{n\,v_{th}}}\right)}. \tag{19}$$

To find the two asymptotes of H_1 we set $\alpha = 0$ in (13) and (14) to yield:

$$H_1 \equiv \frac{I_D^{(-1)}}{I_D^{(0)}} \Rightarrow \frac{1}{m+1}\,(V_G - V_T)\,, \quad \text{for } V_G >> V_T\,, \tag{20}$$

$$\text{and} \qquad \frac{1}{H_1} \equiv \frac{I_D^{(0)}}{I_D^{(-1)}} \Rightarrow \frac{1}{n v_{th}}\,, \quad \text{for } V_G << V_T. \tag{21}$$

Comparison of (18) and (21) indicates that H_1 and $1/TCR$ become identical at low $V_G \ll V_T$:

$$H_1 \Rightarrow \frac{1}{TCR}\,, \quad \text{for } V_G << V_T. \tag{22}$$

Likewise, comparison of (17) and (20) reveals that H_1 and $1/TCR$ are related at high $V_G \gg V_T$ by a constant stipulated by the monomial's order m:

$$H_1 \Rightarrow \frac{m}{m+1}\frac{1}{TCR}\,, \quad \text{for } V_G >> V_T\,, \tag{23}$$

Fig. 3 illustrates the application of both the $v_{th}TCR$ and v_{th}/H_1 auxiliary functions, applying (16) and (19), to the synthetic transfer characteristics of the test hypothetical MOSFET used in Fig. 1. At low $V_G < V_T$ both curves converge to the correct value of the reciprocal $1/n = 1/5$, as expected from their asymptotes respectively defined in (18) and (21). Thus in general, and according to (14), the sub-threshold parameter n ($SS = \ln(10)\, nv_{th}$) may be directly extracted from the constant value that any successive operator ratio $I_D^{(\alpha-1)}/I_D^{(\alpha)}$ should reach below threshold.

Fig. 4 presents the reciprocals of the same two successive operator ratios shown in Fig. 3. As expected, the curves in Fig. 4 reach the correct value of n below threshold ($n = 5$ in this example), and also exhibit the expected linear behavior above threshold with correct slopes of $1/m = 1/2$ and $1/(m+1) = 1/3$ ($m = 2$ in this example). Therefore according to (13) any successive operator ratio of the type $I_D^{(\alpha-1)}/I_D^{(\alpha)}$ can be plotted versus V_G to extract the monomial's order from its above threshold reciprocal slope ($m-\alpha+1$). For the example at hand, either $1/TCR$ ($\alpha = 1$) or H_1 ($\alpha = 0$) may be used to extract the monomial order from their above threshold reciprocal slopes m and $m+1$, as dictated by (17) and (20), respectively, and shown in Fig. 4.

6.4. Transitional value of threshold voltage

It is clear that either one of the strong conduction straight lines corresponding to the two successive operator ratios ($\alpha = 1$ and $\alpha = 0$), shown for illustrative purposes in Fig. 4, if extrapolated to intercept the V_G axis define the same "extrapolated" value of V_T, which coincides with the expected $V_T = 1$V assumed in this hypothetical example. However any successive operator ratio $I_D^{(\alpha-1)}/I_D^{(\alpha)}$, such as *TCR* or or H_1, can also be used to extract a "transition" type value of V_T, that would physically represent the location of the threshold transition point. Such transitional V_T can be properly defined as the V_G axis location that corresponds to a certain given fraction of the maximum value attained by the operator ratio in the sub-threshold region. For the case of *TCR* a fraction of its maximum in the sub-threshold region has been proposed to define the location of V_T [60,62].

The *TCR* or H_1 auxiliary functions, or in fact any other arbitrary ratio of successive operators $I_D^{(\alpha)}/I_D^{(\alpha-1)}$ defined by (12), could be used for this purpose. To establish in general what fraction of the successive operator ratio maximum value corresponds to $V_G = V_T$, we simply evaluate (12) at $V_G = V_T$ and divide the result by the ratio's maximum value below threshold, which according to (14) is always $= 1/(nv_{th})$ for any successive operator ratio. This fraction of the maximum at $V_G = V_T$ is:

$$fraction = \frac{\left.\frac{I_D^{(\alpha)}}{I_D^{(\alpha-1)}}\right|_{V_G=V_T}}{\frac{1}{n\,v_{th}}} = \frac{\mathrm{Li}_{m-\alpha}(-1)}{\mathrm{Li}_{m-(\alpha-1)}(-1)}. \tag{24}$$

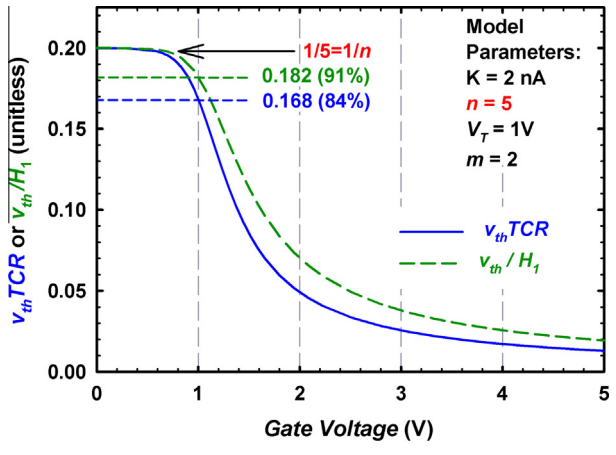

Fig. 3. $v_{th}TCR$ and v_{th}/H_1 of the synthetic characteristics shown in Fig. 1, as calculated using (16) and (19). Both tend to 0.20 below threshold according to (18) and (21), which is the correct value of $1/n$ considering that $n = 5$ in this example.

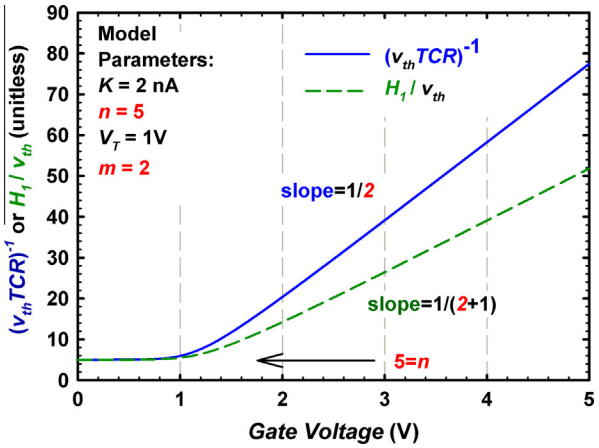

Fig. 4. $(v_{th}TCR)^{-1}$ and H_1/v_{th} of the synthetic characteristics shown in Fig. 1, as calculated using (16) and (19). Both tend to 5 below threshold according to (18) and (21), which is the correct value of n. Above threshold they are linear functions with reciprocal slopes of m and $m+1$, in accordance with (17) and (20), respectively.

Table 1 presents the fraction of below-V_T maximum value of two successive operator ratios, $1/H_1$ and *TCR*, that corresponds to the location of the threshold voltage V_T, for two values of above-V_T monomial order m. In the case of the present example (with $n = 5$, $m = 2$ and $V_T = 1$V), the values of 0.168 and 0.182 shown in Fig. 3 define the location of V_T using either *TCR* or $1/H_1$, respectively. These two numbers correspond to 84% and 91% of the maximum value below threshold of *TCR* and $1/H_1$, respectively.

Again, it is important to keep in mind that this value of V_T, extracted from the location that corresponds to these fractions of the below-V_T maximum, as shown in Fig. 3, is a "transitional" type of V_T value. We must also point out that in this hypothetical example the "transitionally" extracted value of $V_T = 1$V exactly coincides with its "extrapolation" type value of $V_T = 1$V extracted by extrapolating the straight lines shown in Fig. 4.

In conclusion, either *TCR* or H_1, or for that matter any other ratio of successive operators $I_D^{(\alpha)}/I_D^{(\alpha-1)}$ with arbitrary integer value of α as defined by (12), may be directly used to extract the main parameters of this MOSFET's transfer characteristics model: the Subthreshold Swing, $SS = nv_{th}\ln(10)$, the threshold voltage V_T, the strong conduction monomial exponent m, and finally, by back substitution, the coefficient K.

6.5. The "Y" function

Another auxiliary function that is sometimes used for parameter extraction is the Current-to-Square Root of the Transconductance Ratio (CSRTR), for short usually referred to as the "*Y*" function [68]. To the best of our knowledge, this method was independently proposed and originally published in 1988 by Jain [2] and by Ghibaudo [1]. In operator notation the "*Y*" function is:

$$Y \equiv I_D^{(0)} \Big/ \sqrt{I_D^{(1)}}. \tag{25}$$

The motivation underlying the use of such auxiliary function seems to be an attempt to cancel out first order degradation effects of both mobility and source and drain series resistance on the otherwise linear behavior of the above-V_T transfer characteristics, which the method assumes may be described by the following specific function:

$$I_D(V_G) \approx \frac{K}{1+\theta(V_G - V_T)}(V_G - V_T) \qquad \text{for } V_G >> V_T. \tag{26}$$

Here the effective mobility is specifically described by an elementary level first order mobility degradation model which is simply characterized by the factor θ, that includes the mobility degradation and the parasitic resistance effects. Dividing the drain current by the square root of the transconductance in (25) serves the purpose of canceling those effects [69,70]. Once the degradation effects are canceled out, the resulting "*Y*" function is supposed to become a straight line for $V_G \gg V_T$, which can be then extrapolated to intersect the V_G axis at $V_G = V_T$ [71].

However, as Fig. 5 indicates, this method works well only as long as the total degradation effects may be adequately approximated by a first order model such as (26). Otherwise the result of calculating the "*Y*" function will inevitably result in a power function-type curve (a monomial with $m \neq 1$) which may not be linearly extrapolated. Recently, a clever new method has been proposed to linearize and thus improve the extraction precision of the "*Y*" function method [72]. The proposed procedure, which has been applied to organic thin-film transistors (OTFTs) operating in the linear regime, entails sequentially calculating the "*Y*" function and then its H_1 function. The linearity of the resulting curve allows for the extraction of the threshold voltage and the mobility of the OTFT [73].

Table 1
Fraction of below-V_T maximum value that according to (24) corresponds to $V_G = V_T$, for two successive operator ratios ($1/H_1$ and *TCR*) and two values of above-V_T monomial order m.

Ratio	$m = 1$	$m = 2$
$\alpha = 0$ ($1/H_1$)	$12\ln(2)/\pi^2 \approx 0.84$	$\pi^2/(9\,\zeta(3)) \approx 0.91$
$\alpha = 1$ (*TCR*)	$1/(2\ln(2)) \approx 0.72$	$12\ln(2)/\pi^2 \approx 0.84$

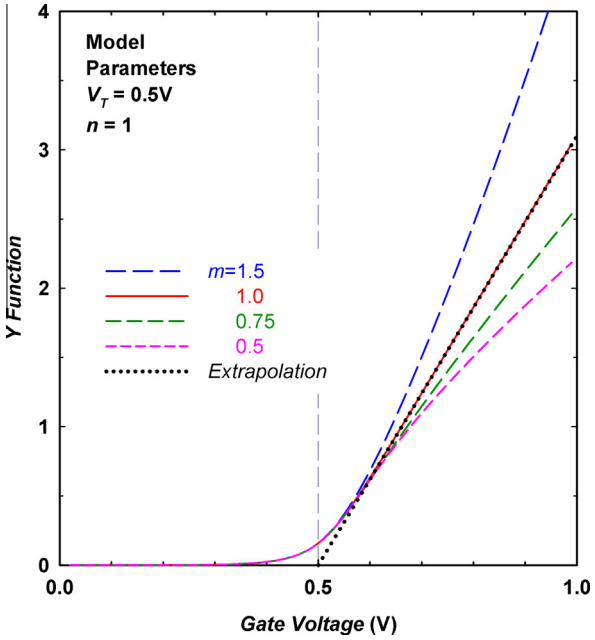

Fig. 5. Y function calculated according to (25) with the same $n = 1$ and $V_T = 0.5$ V, for four different values of the monomial order parameter m. When the above-V_T current is well described by a monomial-like function, this method can cancel out the effects of mobility degradation only if the monomial order is very close to unity ($m \approx 1$) (equivalent to $\theta = 0$ in (26)). In such case the resulting Y function is a straight line for $V_G \gg V_T$, which may be extrapolated to intersect the V_G axis at $V_G = V_T$.

7. Extraction procedures based on triplets of successive operators

A straightforward interpretation of what the conceptual motivations are for using either *TCR* or H_1, readily suggests further parameter extraction procedural possibilities, that could be assembled by combining certain ratios, and which might be useful to isolate some parameters from the effects of others. We exemplify below some of these possibilities.

7.1. Monomial order extraction

A potentially useful auxiliary function may be constructed by multiplying two ratios of successive operators to form a generalized triplet of operators with successive orders of $\alpha - 2$, $\alpha - 1$, and α, as described below:

$$\frac{I_D^{(\alpha)}}{I_D^{(\alpha-1)}}\frac{I_D^{(\alpha-2)}}{I_D^{(\alpha-1)}} = \frac{I_D^{(\alpha)}I_D^{(\alpha-2)}}{I_D^{(\alpha-1)\,2}} = \frac{m-(\alpha-1)}{m-(\alpha-2)} \qquad \text{for } V_G >> V_T. \tag{27}$$

Application of (27) to a MOSFET's measured transfer characteristics allows extracting the value of parameter m independently of K and V_T, and irrespectively of the value of α chosen. Solving (27)

yields a closed form general formula for the reciprocal of the above-V_T monomial order m that is independent of all the other parameters in the model:

$$\frac{1}{m} = \frac{\frac{I_D^{(\alpha-1)\,2}}{I_D^{(\alpha)} I_D^{(\alpha-2)}} - 1}{(\alpha-1)\frac{I_D^{(\alpha-1)\,2}}{I_D^{(\alpha)} I_D^{(\alpha-2)}} - (\alpha-2)} \qquad \text{for } V_G >> V_T. \tag{28}$$

As it might be evident by now, in the above formulas α now indicates the largest order of the three successive operator orders $(\alpha-2, \alpha-1, \alpha)$ present in the triplet. The value of α in the triplet may be any real integer. The actual value chosen is totally up to us, although the decision should be based on practical considerations to be discussed later.

An interesting case results by setting the largest order operator $\alpha = 1$. Doing so turns triplet (27) into the product of two already familiar ratios, *TCR* and H_1:

$$TCR\,H_1 \equiv \frac{I_D^{(1)}}{I_D^{(0)}}\frac{I_D^{(-1)}}{I_D^{(0)}} = \frac{I_D^{(1)} I_D^{(-1)}}{I_D^{(0)\,2}} = \frac{m}{m+1} \qquad \text{for } V_G >> V_T, \tag{29}$$

which can be solved for the reciprocal of m to yield:

$$\frac{1}{m} = \frac{I_D^{(0)\,2}}{I_D^{(1)} I_D^{(-1)}} - 1 \qquad \text{for } V_G >> V_T. \tag{30}$$

Fig. 6 shows two examples of the application of Eq. (28) to the synthetic characteristics shown in Fig. 1, using differentiation (a triplet with $\alpha = 2$), and integration (a triplet with $\alpha = -1$). In both cases the resulting auxiliary function tends to the expected value of $1/m = 1/2$ at high values V_G.

7.2. Extraction of the threshold voltage

A closed form general formula for V_T might be obtained from the above-V_T monomials of order m of the ratio of two successive operators, described by (13):

$$V_T = V_G - (m - \alpha + 1)\frac{I_D^{(\alpha-1)}}{I_D^{(\alpha)}}, \quad \text{for } V_G >> V_T, \tag{31}$$

Regardless of the value of α chosen, combining (28) and (31) provides a formula to extract the value of V_T independently of the values of K and m:

$$V_T = V_G - \left(\frac{(\alpha-1)\frac{I_D^{(\alpha-1)\,2}}{I_D^{(\alpha)} I_D^{(\alpha-2)}} - (\alpha-2)}{\frac{I_D^{(\alpha-1)\,2}}{I_D^{(\alpha)} I_D^{(\alpha-2)}} - 1} - \alpha + 1 \right) \frac{I_D^{(\alpha-1)}}{I_D^{(\alpha)}}, \quad \text{for } V_G >> V_T. \tag{32}$$

Fig. 7 shows two examples of the application of Eq. (32) to the synthetic characteristics shown in Fig. 1, as calculated using differentiation (a triplet with $\alpha = 2$), and integration (a triplet with $\alpha = -1$). In both cases the resulting auxiliary function tend to the expected value of $V_T = 1$ at high V_G values.

7.3. Choosing the successive operator order

In principle we are at liberty of arbitrarily choosing the largest operator order α in the triplet, since theoretically no particular triplet offers advantages over another. However, this is not the case once we recall that the actual operations to be carried out (derivatives and/or integrals) are numerical calculations that must be performed in real practice within the terms imposed by experimentally measured data. Therefore, the question of the best choice for triplet maximum order remains relevant.

Considering actual practical implementation, there are essentially two criteria to consider for maximum order selection. The first concerns computational efficiency and obviously translates into a recommendation to perform the least number of operations (numerical computations) possible. Hence, the best choice would be any successive operator triplet that contains the function itself ($\alpha = 0$, $I_D^{(0)}$), because that way only two numerical computations would be required. There are three such possible triplets: those whose maximum operator order is $\alpha = 0$, 1 or 2. These values of α correspond to triplets: $(-2,-1,0)$ with only two integrations; $(-1,0,1)$ with one integration and one differentiation; and $(0,1,2)$ with two differentiations.

A second criterion for selecting a triplet's maximum operator order involves the issue of data noise. Experience suggests that raw measured data likely contains significant measurement noise, especially at low gate voltages. Since differentiation would enhance noise, most likely also increasing the extraction error, direct differentiation of raw noisy transfer characteristics should be avoided. Therefore, additional data smoothing operations must be necessarily included in the procedure if numerical differentiation is contemplated. In any event, from a noise reduction point of view it would be generally advisable to try to reduce, or

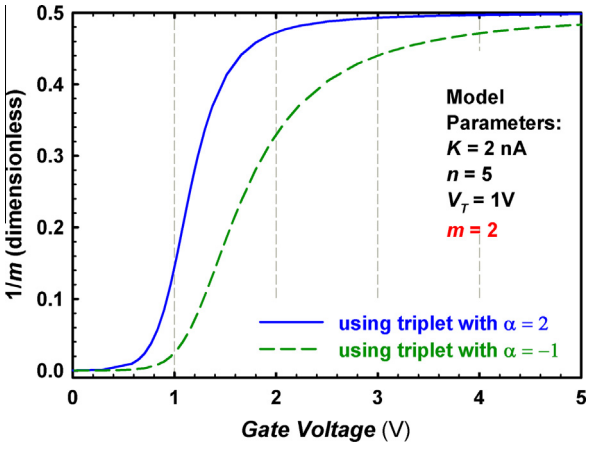

Fig. 6. Two examples of extracting m by applying (28) to the synthetic characteristics of the device of Fig. 1, calculated using triplet with $\alpha = 2$ (differentiation) (continuous line) and triplet with $\alpha = -1$(integration) (dashed line). Both triplets tend to the correct value of $1/m = 0.5$ al high values of V_G.

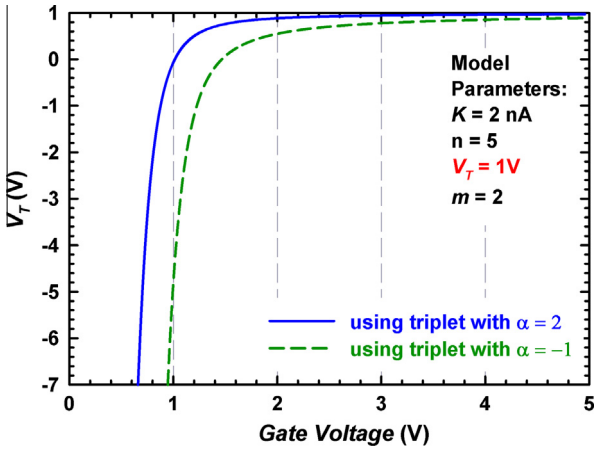

Fig. 7. Two examples of extracting V_T by applying (32) to the same synthetic characteristics of the device of Fig. 1, calculated using $\alpha = 2$ (differentiation) (continuous line) and $\alpha = -1$(integration) (dashed line). Both curves tend to the correct value of $V_T = 1$ V al high values of V_G.

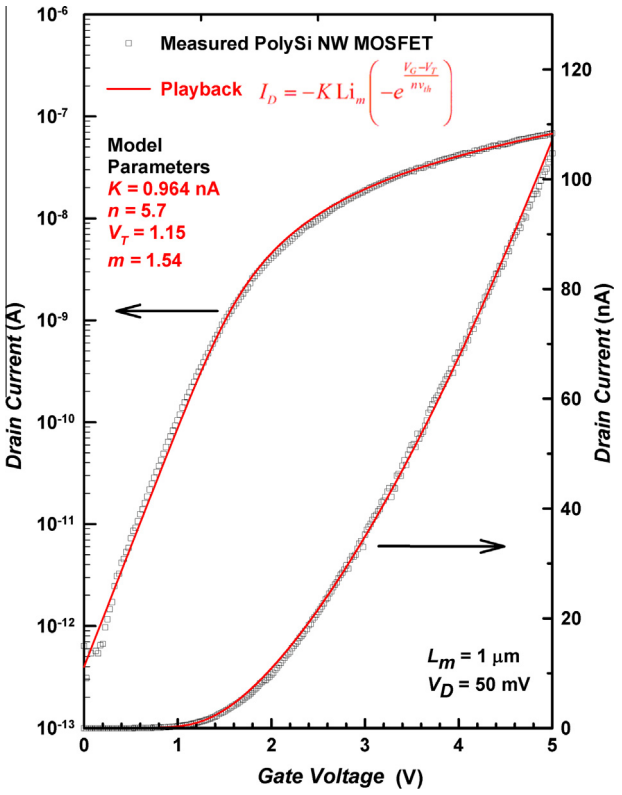

Fig. 8. Measured transfer characteristics of a PolySi NW MOSFET in the linear region (square symbols) and model playback (solid lines) calculated using (6) with the extracted parameter values indicated within the figure.

altogether avoid, operators of order $\alpha > 0$. And since, on the other hand, integration inherently reduces noise without additional data smoothing operations, from the same point of view it would be generally advisable to try to use operators of order $\alpha < 0$. Hence, the best alternative according to this criterion seems to be the use of three successive integral operators. Setting the triplet's maximum order to $\alpha = -1$ results in triplet $(-3,-2,-1)$, which corresponds to using the first three successive integral operators $I_D^{(-1)}$, $I_D^{(-2)}$ and $I_D^{(-3)}$.

Notwithstanding the above, whenever the available data is not particularly noisy, such as when dealing with synthetic characteristics or previously smoothed measured data, the noise-reduction criterion for operator order choice could be ignored altogether. In such cases a good option to minimize the numerical computational burden would be setting the maximum operator order to $\alpha = 2$, resulting in triplet $(0,1,2)$, which corresponds to using the original function $I_D^{(0)}$ together with its first $I_D^{(1)}$ and second $I_D^{(2)}$ successive derivatives.

8. Examples of extraction from real device transfer characteristics

We illustrate now the use of some of the extraction procedures by applying them to the transfer characteristics of an experimental PolySi NW MOSFET measured in the linear regions at $V_D = 50$ mV, as shown in Fig. 8. This device was previously modeled by us using a different Lambert*W* function-based model [38,45], but will now assume here that the measured transfer characteristics of this device can also be adequately described by the presently proposed simple polylogarithmic model given by (1). Therefore, here we will attempt to extract this model's four basic parameters: n, m, V_T and K, by applying some of the already discussed extraction procedures to this device's transfer characteristics shown in Fig. 8.

8.1. Using successive operator ratios

The Transconductance-to-Current Ratio (TCR) is obtained by setting $\alpha = 1$ in (12) to yield expression (16). Fig. 9 presents the result of numerically calculating the $v_{th}TCR$ from the data of this experimental device, shown in Fig. 8. According to (18) we should be able to extract the value of n from the low voltage asymptote of the below-threshold $v_{th}TCR$ curve shown in Fig. 9. However, without attempting any smoothing scheme of the raw measured data, it seems in this particular case that the noise present is sufficiently high to obscure the extraction of n from that region.

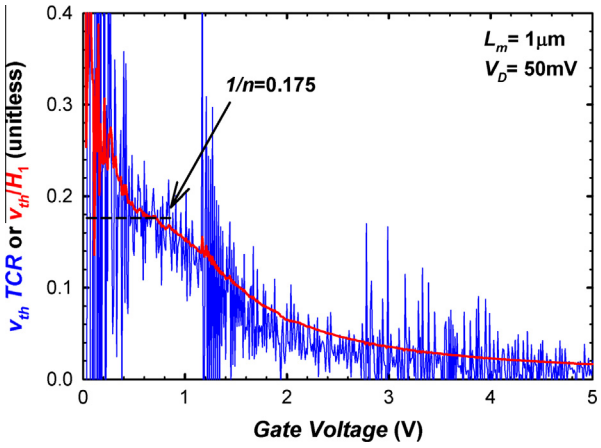

Fig. 9. Transconductance-to-Current Ratio ($v_{th}TCR$) (thin blue line) and inverse v_{th}/H_1 function (thick red line) of a PolySi NW MOSFET transfer characteristics measured at $V_D = 50$ mV, shown in Fig. 8, as numerically calculated using (16) and (19). According to (18) or (21) the below-V_T low V_G asymptote yields the value of $1/n$. In spite of the large noise present, it is still possible to estimate that the curves tend to about 0.175, which means that $n \approx 5.7$, equivalent to SS = 340 mV/dec at $T = 300$ K. It is obvious that using v_{th}/H_1 instead of $v_{th}TCR$ greatly reduces the extraction uncertainty due to noise. (For interpretation of the references to colour in this figure legend, the reader is referred to the web version of this article.)

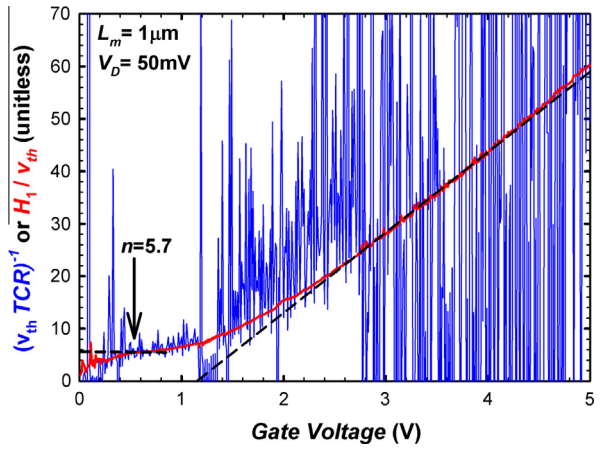

Fig. 10. $1/(v_{th}TCR)$ (thin blue line) and H_1/v_{th} (thick red line) of a PolySi NW MOSFET transfer characteristics measured at $V_D = 50$ mV, shown in Fig. 8, as numerically calculated using (16) and (19). According to (17) or (20) the slope of the above-threshold high V_G asymptote gives the value of $1/m$ or $1/(m+1)$ and its extrapolated V_G axis intercept gives V_T. In spite of the large noise present, it is still possible to estimate $m \approx 1.54$, and $V_T \approx 1.15$ V from the high V_G asymptote of H_1 (dash black line). (For interpretation of the references to colour in this figure legend, the reader is referred to the web version of this article.)

Instead of the $v_{th}TCR$, we could use the v_{th}/H_1 function, obtained by setting $\alpha = 0$ in (12) to yield expression (20). Fig. 9 also presents the result of numerically calculating v_{th}/H_1 from the data of this experimental device, shown in Fig. 8. According to (21) we should be able to extract the value of n from the low voltage asymptote of v_{th}/H_1 shown in Fig. 9.

Unfortunately, even using the v_{th}/H_1 curve, the considerable noise present at low V_G below-V_T in this experimental device only allows us to get from Fig. 9 a very rough estimate of the value of $1/n \approx 0.175$, corresponding to $n \approx 5.7$, which represents an $SS = nv_{th}\ln(10) \approx 340$ mV/dec, at standard $T = 300$ K ($v_{th} = 0.0259$ V).

Fig. 10 presents the reciprocals of the two functions presented in Fig. 9, that is, $1/(v_{th}TCR)$ and H_1/v_{th} as calculated from the transfer characteristics measured at $V_D = 50$ mV, shown in Fig. 8. According to (17) or (20) the slopes of the above-V_T asymptotes at high V_G yields the values of $1/m$ or $1/(m+1)$, respectively, and their extrapolations to the V_G axis yields the value of V_T. We observe that the large noise present precludes the use of the differentiation based auxiliary function $1/(v_{th}TCR)$.

However, it is still possible to use the H_1/v_{th} high V_G asymptote to estimate $m \approx 1.54$, and $V_T \approx 1.15$V. This example clearly illustrates that using H_1/v_{th} instead of $1/(v_{th}TCR)$ greatly reduces the extraction uncertainty that arises from measurement noise.

We could also extract a transition type value of V_T from the low V_G regions of $v_{th}TCR$ and v_{th}/H_1 graphs in Fig. 9. According to (24), V_T is the location on the V_G axis corresponding to a given fraction of either functions' maximum measured at low V_G. Calculating that fraction of the maximum of $v_{th}TCR$ or v_{th}/H_1 in Fig. 9 for a value of $m \approx 1.54$ using (24), the fractions corresponds in either case to a value of $V_T \approx 1.15$V.

The value of the specific current parameter K is finally extracted by back substitution into the model equation. With the already extracted three basic parameters n, m, and V_T, the fourth, K, is calculated to be in this example: $K \approx 0.964$ nA.

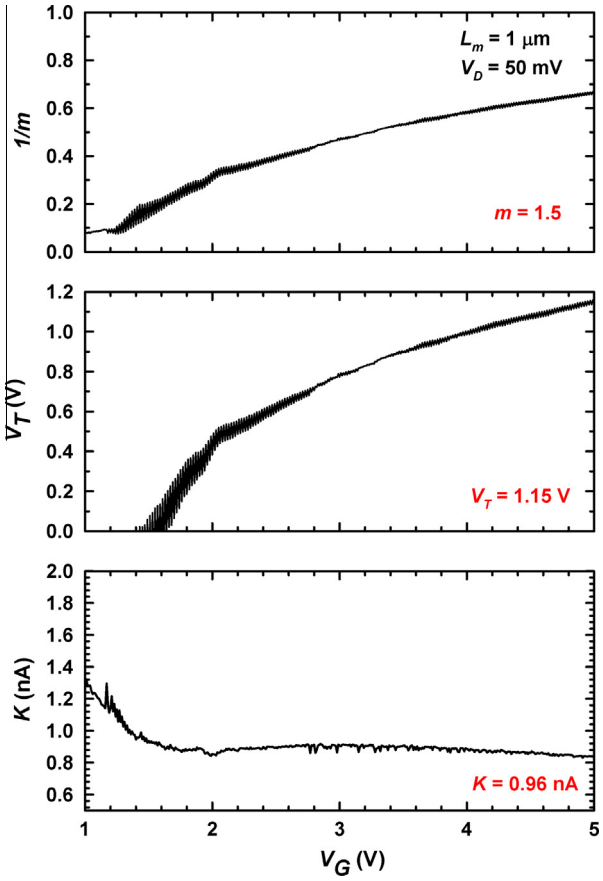

Fig. 11. Evolution of m and V_T as functions of gate voltage, for the PolySi NW MOSFET transfer characteristics measured at $V_D = 50$ mV, shown in Fig. 8. An integration-only successive operator triplet with $\alpha = 0$ was used for calculating $1/m$ with (28).

8.2. Using successive operator triplets

Monomial order m and threshold voltage V_T may also be extracted using the direct formulas given by expressions (28) and (32) respectively. Fig. 11 presents m and V_T, as functions of gate voltage for $V_G \gg V_T$, setting $\alpha = 0$ in (28) to use an integration-only successive operator triplet. The value of K shown in Fig. 11 was calculated by back substitution and used together with the other already extracted three parameters n, m, and V_T to generate the model playback shown in Fig. 8 superimposed on the originally measured data. Notice in Fig. 11 the constancy of K above threshold.

9. Classification of successive operator methods

The generalized auxiliary functions described and discussed here represent only some examples of how successive differential and integral operators, their ratios, and other combinations thereof, may be advantageously used for the important task of MOSFET model parameter extraction. Conceivably, other procedures could be similarly assembled to extract model parameters on the basis of other combinations of appropriate operators, operator ratios, operator triplets, and ultimately by back substitution into the original model. The diversity of MOSFET model parameter extraction applications that are presently available utilizing successive differentiation and integration is portrayed in Table 2.

Notice that Table 2 includes two rows corresponding to two conceptually different threshold voltage parameters, referring to the value extracted by extrapolation and that extracted from the threshold transition region itself. The specific current parameter K is not shown in Table 2 because it is usually extracted by back substitution in a final procedural step.

Different extraction procedures frequently yield different values of the model parameters of a given assumed model. The accuracy of the extracted values is highly dependent upon the following principal factors: (a) the appropriateness of the assumed model to satisfactory describe the transfer characteristics being analyzed,

Table 2
Classification of successive differentiation and integration-based techniques for MOSFET model parameter extraction, according to the model parameter intended to be extracted.

Parameter intended to be extracted	Type of technique					
	Single operator (order)			Operator ratio		Operator triplet
	Zero	First	Higher	Differential	Integral	
Sub-threshold n		X		X	X	X
Threshold voltage V_T (Extrapolated)		X	X	X	X	X
Threshold voltage V_T (Transition)	X		X	X	X	
Supra-threshold m				X	X	X

(b) the adequacy of the extraction procedure chosen to isolate the parameter being sought in the assumed model, (c) the validity of the assumptions presumed to hold by the extraction procedure to be applied, (d) the nature of the actual numerical calculation methods used, including the noise-canceling algorithms.

Nevertheless, even when the extracted parameter values may not be considered to be exact and uniquely defined quantities, most extracted parameters, regardless of the particular extraction scheme used, would still be useful as coarse indicators of the MOSFET's performance, because any extracted parameter is likely to exhibit a generally correct correlation with the device's structural characteristics and underlying physical phenomena.

10. Conclusions

We have presented a unified comparative analysis of how successive differential and integral operators are used in procedures to extract MOSFET model parameters. The analysis was based on assessing the ability of the operators, their ratios and other combinations to extract the basic model parameters of a simple minimalist four-parameter empiric model of MOSFET transfer characteristics.

The model is a novel mathematical description of drain current continuously from depletion to strong inversion, based on a polylogarithm function of gate voltage. This model's exponential- and monomial-type low and high gate voltage asymptotes, respectively, are used for extraction since they describe reasonable well the general below- and above-threshold drain current behavior of MOSFETs. Although monomial-type descriptions of strong inversion behavior have been traditionally reserved for non-crystalline MOSFETs, for the sake of the present comparative analysis, we have extended monomial portrayal to other types of FETs as a sufficiently adequate way for describing their above-threshold behavior. The use of this concise model has allowed us to analyze and compare in a consistent manner the existing most significant and better known extraction schemes that are based on successive differential and integral operators and their ratios.

Additionally, we have explored other potentially promising extraction ideas that go beyond the simple use of successive operators and their ratios. We have briefly discussed the choice of successive operator order from the perspective of computational efficiency and noise reduction. Finally, we have illustrated with real examples the application of some successive operator-based procedures to extract the basic model parameters from measured transfer characteristics of experimental PolySi NW MOSFETs.

The joint parallel depiction of differential and integral operators and their ratios that we have presented here provides a singular systematic overview of their use in existing model parameter extraction procedures. This type of vision facilitates conceiving other combinations that may result useful in the future.

Acknowledgments

The authors thank Horng-Chih Lin of the National Chiao Tung University, Hsinchu, Taiwan, for providing the experimental PolySi NW MOSFETs used for the illustrative examples presented here.

Appendix A

Some characteristics of the polylogarithm function pertaining to this work [33].

A.1. Definitions

The polylogarithm is a special function defined for any arbitrary order m as the infinite power series:

$$\mathrm{Li}_m(z) = \sum_{k=1}^{\infty} k^{-m} z^k, \tag{A1.1}$$

which is valid for all $|z| < 1$, but can be extended for $|z| \geqslant 1$ by analytic continuation.

The polylogarithm may also be expressed in terms of the integral:

$$\mathrm{Li}_m(z) = \frac{1}{\Gamma(m)} \int_0^{\infty} \frac{t^{m-1}}{\frac{e^t}{z} - 1} dt. \tag{A1.2}$$

$$\text{Letting } z = -e^u: \quad -\mathrm{Li}_m(-e^u) = -\frac{1}{\Gamma(m)} \int_0^{\infty} \frac{t^{m-1}}{e^{t-u} + 1} dt, \tag{A1.3}$$

The integrand of (A1.3) is the Fermi–Dirac distribution. Thus we may write:

$$-\mathrm{Li}_m(-e^u) = F_{m-1}(u), \tag{A1.4}$$

where $F_{m-1}(u)$ is the complete Fermi–Dirac integral of order $m - 1$.

A.2. The polylogarithm in terms of elementary functions

When the order of the polylogarithm is an integer $m \leqslant 1$, it may be expressed in terms of elementary functions:

$$\text{For } m = -2: \quad \mathrm{Li}_{-2}(z) = \frac{z^2 + z}{(1 - z)^3}. \tag{A2.1}$$

$$\text{Letting } z = -e^u: \quad -\mathrm{Li}_{-2}(-e^u) = \frac{e^u - e^{2u}}{(1 + e^u)^3}. \tag{A2.2}$$

Notice that the above function vanishes when $u = 0$ (the argument becomes -1):

$$-\mathrm{Li}_{-2}(-e^u)|_{u=0} = -\mathrm{Li}_{-2}(-1) = 0. \tag{A2.3}$$

$$\text{For } m = -1: \quad \mathrm{Li}_{-1}(z) = \frac{z}{(1 - z)^2}. \tag{A2.4}$$

$$\text{Letting } z = -e^u: \quad -\mathrm{Li}_{-1}(-e^u) = \frac{e^u}{(1 + e^u)^2}. \tag{A2.5}$$

$$\text{For } m = 0: \quad \mathrm{Li}_0(z) = \frac{z}{1 - z}. \tag{A2.6}$$

$$\text{Letting } z = -e^u: \quad -\mathrm{Li}_0(-e^u) = \frac{1}{e^{-u} + 1}. \tag{A2.7}$$

$$\text{For } m = 1: \quad \mathrm{Li}_1(z) = -\ln(1 - z). \tag{A2.8}$$

$$\text{Letting } z = -e^u: \quad -\mathrm{Li}_1(-e^u) = \ln(1 + e^u). \tag{A2.9}$$

Notice that the expression corresponding to $m = 1$ defined in (A2.8) by elementary functions tends asymptotically to e^u for values of $u \ll 0$ and to u for values of $u \gg 0$. Because of this distinctive attribute, it has been frequently used in electron device modeling applications to portray a phenomenological transition at $u = 0$ from an exponential-like behavior to a linear-like behavior [74,75].

A.3. Derivatives of the polylogarithm

$$\frac{\partial \mathrm{Li}_m(z)}{\partial z} = \frac{1}{z} \mathrm{Li}_{m-1}(z). \tag{A3.1}$$

$$\text{Let } z = f(u) \qquad \frac{\partial \mathrm{Li}_m(f(u))}{\partial u} = \frac{1}{f(u)} \frac{\partial f(u)}{\partial u} \mathrm{Li}_{m-1}(f(u)). \tag{A3.2}$$

$$\text{Letting } f(u) = -e^u: \quad \frac{\partial \mathrm{Li}_m(-e^u)}{\partial u} = \mathrm{Li}_{m-1}(-e^u). \tag{A3.3}$$

A.4. Some particular values of the polylogarithm

Values of the polylogarithm of argument $z = -1$ for different values of its order m:

$$\text{For } m = -2 \quad \mathrm{Li}_{-2}(-1) = 0. \tag{A4.1}$$

$$\text{For } m = 1 \quad \mathrm{Li}_{1}(-1) = -\ln(2). \tag{A4.2}$$

$$\text{For } m > 1 \quad \mathrm{Li}_{m}(-1) = -\eta(m) = \left(2^{1-m} - 1\right)\zeta(m), \tag{A4.3}$$

where $\eta(\cdot)$ is the Eta function and $\zeta(\cdot)$ is the Riemann Zeta function [51].

References

[1] Ghibaudo G. New method for the extraction of MOSFET parameters. Electr Lett 1988;24:543–5.
[2] Jain S. Measurement of threshold voltage and channel length of submicron MOSFETs. IEE Proc I: Solid-State and Electron Dev 1988;135:162–4. http://dx.doi.org/10.1049/ip-i-1.1988.0029.
[3] Aoyama K. A method for extracting the threshold voltage of MOSFETs based on current components. Simul Semicond Devices Processes 1995;6:118–21. http://dx.doi.org/10.1007/978-3-7091-6619-2_28.
[4] Liou JJ, Ortiz-Conde A, García-Sánchez FJ. Analysis and design of MOSFETs: modeling, simulation and parameter extraction. New York: Springer; 1998, ISBN 978-0-412-14601-5.
[5] Terada K, Nishiyama K, Hatanaka K-I. Comparison of MOSFETthreshold-voltage extraction methods. Solid-State Electronics 2001;45:35–40. http://dx.doi.org/10.1016/S0038-1101(00)00187-8.
[6] Schroeder DK. Semiconductor material and device characterization. 3rd ed. New York: Wiley; 2006, ISBN 978-0-471-74908-0.
[7] Galup-Montoro C, Schneider MC. Mosfet modeling for circuit analysis and design. International Series on Advances in Solid State Electronics and Technology, World Scientific; 2007, ISBN 978-981-256-810-6.
[8] Deen MJ, Marinov O, Zschieschang U, Klauk H. Organic thin film transistors: Part II- parameter extraction. IEEE Trans Electron Dev 2009;56:2962–8. http://dx.doi.org/10.1109/TED.2009.2033309.
[9] Tsormpatzoglou A, Papathanasiou K, Fasarakis N, Tassis DH, Ghibaudo G, Dimitriadis CA. A Lambert-function charge-based methodology for extracting electrical parameters of nanoscale FinFETs. IEEE Trans Electron Dev 2012;59:3299–305. http://dx.doi.org/10.1109/TED.2012.2222647.
[10] Ortiz-Conde A, García-Sánchez FJ, Muci J, Terán Barrios A, Liou JJ, Ho C-S. Revisiting MOSFET threshold voltage extraction methods. Microelectron Reliab 2013;53:90–104. http://dx.doi.org/10.1016/j.microrel.2012.09.015.
[11] Ortiz-Conde A, García-Sánchez FJ, Muci J, Sucre-González A, Martino JA, Der Agopian PG, et al. Threshold voltage extraction in tunnel FETs. Solid-State Electron 2014;93:49–55. http://dx.doi.org/10.1016/j.sse.2013.12.010.
[12] Ramm AG, Smirnova AB. On stable numerical differentiation. Math Comput 2001;70:1131–53.
[13] Choi WY, Kim H, Lee B, Lee JD, Park B-G. Stable threshold voltage extraction using Tikhonov's regularization theory. IEEE Trans Electron Dev 2004;51:1833–9. http://dx.doi.org/10.1109/TED.2004.837010.
[14] Ibáñez MJ, Roldán JB, Roldán AM, Yáñez R. A comprehensive characterization of the threshold voltage extraction in MOSFETs transistors based on smoothing splines. Math Comput Simul 2014;102:1–10. http://dx.doi.org/10.1016/j.matcom.2013.04.024.
[15] Ranuarez JC, García-Sánchez FJ, Ortiz-Conde A. Procedure for the determination of diode model parameters at very low forward voltage. Solid-State Electron 1999;43:2129–33. http://dx.doi.org/10.1016/S0038-1101(99)00181-1.
[16] Cerdeira A, Estrada M, García R, Ortiz-Conde A, García-Sánchez FJ. New procedure for the extraction of basic a-Si:H TFT model parameters in the linear and saturation regions. Solid-State Electron 2001;45:1077–80. http://dx.doi.org/10.1016/S0038-1101(01)00143-5.
[17] Ortiz-Conde A, García Sánchez FJ. Extraction of non-ideal junction model parameters from the explicit analytic solutions of its *I–V* characteristics. Solid-State Electron 2005;49:465–72. http://dx.doi.org/10.1016/j.sse.2004.12.001.
[18] Ortiz-Conde A, García Sánchez FJ, Muci J. New method to extract the model parameters of solar cells from the explicit analytic solutions of their illuminated *I–V* characteristics. Solar Energy Mater Solar Cells 2006;90:352–61. http://dx.doi.org/10.1016/j.solmat.2005.04.023.
[19] Ortiz-Conde A, García Sánchez FJ, Muci J. New method to extract the model parameters of solar cells from the explicit analytic solutions of their illuminated *I–V* characteristics. Solar Energy Mater Solar Cells 2006;90:352–61. http://dx.doi.org/10.1016/j.solmat.2005.04.023.
[20] Ortiz-Conde A, García Sánchez FJ, Salazar R. On integration-based methods for MOSFET model parameter extraction. In: 9th Int Conf on Solid-State and Integrated-Circuit Technol (ICSICT), Beijing, China, October 2008. <http://dx.doi.org/10.1109/ICSICT.2008.4734566>.
[21] Muci J, Lugo-Muñoz D, Latorre-Rey A, Ortiz-Conde A, García Sánchez FJ, Ho C-S, et al. A new integration-based procedure to separately extract series resistance and mobility degradation in MOSFETs. Semicond Sci Technol 2009;24:105015. http://dx.doi.org/10.1088/0268-1242/24/10/105015. p. 6.
[22] Ortiz-Conde A, García-Sánchez FJ, Liou JJ, Ching-Sung Ho. Integration-based approach to evaluate the sub-threshold slope of MOSFETs. Microelectron Reliabil 2010;50:312–5. http://dx.doi.org/10.1016/j.microrel.2009.11.001.
[23] Ortiz-Conde A, Latorre Rey AD, Liu W, Chen W-C, Lin H-C, Liou JJ, et al. Parameter extraction in polysilicon nanowire MOSFETs using new double integration-based procedure. Solid-State Electron 2010;54:635–41. http://dx.doi.org/10.1016/j.sse.2010.01.011.
[24] García-Sánchez FJ, Ortiz-Conde A, De Mercato G, Salcedo JA, Liou JJ, Yue Y. New simple procedure to determine the threshold voltage of MOSFETs. Solid-State Electron 2000;44:673–5. http://dx.doi.org/10.1016/S0038-1101(99)00254-3.
[25] Cerdeira A, Estrada M, Quintero R, Flandre D, Ortiz-Conde A, García-Sánchez FJ. New method for determination of harmonic distortion in SOI FD transistors. Solid-State Electron 2002;46:103–8. http://dx.doi.org/10.1016/S0038-1101(01)00258-1.
[26] Salazar R, Ortiz-Conde A, García Sánchez FJ, Ho C-S, Liou JJ. Evaluating MOSFET harmonic distortion by successive integration of the *I–V* characteristics. Solid-State Electronics 2008;52:1092–8. http://dx.doi.org/10.1016/j.sse.2008.03.018.
[27] Salazar R, Ortiz-Conde A, García Sánchez FJ. Harmonic distortion in MOSFETs calculated by successive integration of the transfer characteristics. In: 9th Int Conf on Solid-State and Integrated-Circuit Technol (ICSICT), Beijing, China, October 2008. <http://dx.doi.org/10.1109/ICSICT.2008.4734556>.
[28] Bissels GMMW, Schermer JJ, Asselbergs MAH, Haverkamp EJ, Mulder P, et al. Theoretical review of series resistance determination methods for solar cells. Solar Energy Mater Solar Cells 2014;130:605–14. http://dx.doi.org/10.1016/j.solmat.2014.08.003.
[29] Keller S, Harris DM, Martin AJ. A compact transregional model for digital CMOS circuits operating near threshold. IEEE Trans VLSI Syst 2014;22(10):2041–53. http://dx.doi.org/10.1109/TVLSI.2013.2282316.
[30] Lee S, Striakhilev D, Jeon S, Nathan A. Unified analytic model for current–voltage behavior in amorphous oxide semiconductor TFTs. IEEE Electron Dev Lett 2014;35(1):84–6. http://dx.doi.org/10.1109/LED.2013.2290532.
[31] Eimori T, Anami K, Yoshimatsu N, Hasebe T, Murakami K. Analog design optimization methodology for ultralow-power circuits using intuitive inversion-level and saturation-level parameters. Japan J Appl Phys 2014;53:04EE23. http://dx.doi.org/10.7567/JJAP.53.04EE23.
[32] Marinov O, Deen MJ, Zschieschang U, Klauk H. Organic thin-film transistors: Part I – compact DC modeling. IEEE Trans Electron Dev 2009;56:2952–61. http://dx.doi.org/10.1109/TED.2009.2033308.
[33] Polylogarithms, Zeta and Related Functions. NIST digital library of mathematical functions (online), <http://dlmf.nist.gov/25.12>.
[34] Kim R, Lundstrom M. Notes on Fermi–Dirac integrals. In: Network for computational nanotechnology. Purdue University; 2008. <https://www.nanohub.org/resources/5475/>.
[35] Chaudhry MA, Qadir A. Operator representations of Fermi–Dirac and Bose–Einstein integral functions with applications. Int J Math Mathematical Sci 2007;80515:1–8. http://dx.doi.org/10.1155/2007/80515.
[36] Ulrich MD, Seng WF, Barnes PA. Solutions to the Fermi–Dirac integrals in semiconductor physics using polylogarithms. J Comput Electron 2002;1:431–4. http://dx.doi.org/10.1023/A:1020784532229.
[37] Corless RM, Gonnet GH, Hare DEG, Jeffrey DJ, Knuth DE. On the lambert W function. Advan Comput Math 1996;5:329–59. http://dx.doi.org/10.1007/BF02124750.
[38] Lambert W-Function. NIST digital library of mathematical functions (online). <http://dlmf.nist.gov/54.13>.
[39] Temme NM, Olde Daalhius AB. Uniform asymptotic approximation of Fermi–Dirac integrals. J Comp Appl Math 1990;31:383–7. http://dx.doi.org/10.1016/0377-0427(90)90038-2.
[40] Gamma Function. Chapter 5 of NIST digital library of mathematical functions (online). <http://dlmf.nist.gov/5>.
[41] Ortiz-Conde A, Cerdeira A, Estrada M, García-Sánchez FJ, Quintero R. A simple procedure to extract the threshold voltage of amorphous thin film MOSFETs in the saturation region. Solid-State Electron 2001;45:663–7. http://dx.doi.org/10.1016/S0038-1101(01)00123-X.
[42] Marinov O, Deen MJ, Datars R. Compact modeling of charge carrier mobility in organic thin-film transistors. J App Phys 2009;106:064501-01–1-13. http://dx.doi.org/10.1063/1.3212539.
[43] Kumar Singh V, Mazhari B. Measurement of threshold voltage in organic thin film transistors. Appl Phys Lett 2013;102:253304–13. http://dx.doi.org/10.1063/1.4812191.
[44] Kumar B, Kaushik BK, Negi YS, Goswami V. Single and dual gate OTFT based robust organic digital design. Microelectron Reliab 2014;54:100–9. http://dx.doi.org/10.1016/j.microrel.2013.09.015.
[45] García-Sánchez FJ, Latorre-Rey AD, Liu W, Chen W-C, Lin H-C, Liou JJ, et al. A continuous semi-empiric transfer characteristics model for surrounding gate undoped polysilicon nanowire MOSFETs. Solid-State Electron 2011;63:22–6. http://dx.doi.org/10.1016/j.sse.2011.05.004.
[46] White MH, Cricchi JR. Complementary MOS transistors. Solid-State Electron 1966;9:991–1008. http://dx.doi.org/10.1016/0038-1101(66)90075-X.
[47] Zhou X, Lim KY, Lim D. A simple and unambiguous definition of threshold voltage and its implications in deep-submicron MOS device modeling. IEEE Trans Electron Dev 1999;46:807–9. http://dx.doi.org/10.1109/16.753720.
[48] Zhou X, Lim KY, Qian W. Threshold voltage definition and extraction for deep submicron MOSFETs. Solid-State Electron 2001;45:507–10. http://dx.doi.org/10.1016/S0038-1101(01)00035-1.

[49] Bazigos A, Bucher M, Assenmacher J, Decker S, Grabinski W, Papananos Y. An adjusted constant-current method to determine saturated and linear mode threshold voltage of MOSFETs. IEEE Trans Electron Dev 2011;58(1):3751–8. http://dx.doi.org/10.1109/TED.2011.2164080.
[50] Makovejev S, Esfeh BK, Andrieu F, Jean-Pierre Raskin J-P, Flandre D, Kilchytska V. Assessment of global variability in UTBB MOSFETs in subthreshold regime. J. Low Power Electron Appl 2014;4:201–13. http://dx.doi.org/10.3390/jlpea4030201.
[51] Riemann Zeta Function and Incomplete Riemann Zeta Function. Incomplete gamma and related functions. Chapter 8 of NIST digital library of mathematical functions (online). <http://dlmf.nist.gov/8.22>.
[52] Araujo GL, Sánchez E. A new method for experimental determination of the series resistance of a solar cell. IEEETrans Electron Dev 1982;29:1511–3. http://dx.doi.org/10.1109/T-ED.1982.20906.
[53] García-Sánchez FJ, Ortiz-Conde A, Cerdeira A, Estrada M, Flandre D, Liou JJ. A method to extract mobility degradation and total series resistance of fully-depleted SOI MOSFETs. IEEE Trans Electron Dev 2002;49:82–8. http://dx.doi.org/10.1109/16.974753.
[54] García-Sánchez FJ, Ortiz-Conde A, Muci J. Understanding threshold voltage in undoped-body MOSFETs: an appraisal of various criteria. Microelectronics Reliab 2006;46(5–6):731–42. http://dx.doi.org/10.1016/j.microrel.2005.07.116.
[55] Wong HS, White MH, Krutsick TJ, Booth RV. Modeling of transconductance degradation and extraction of threshold voltage in thin oxide MOSFETs. Solid-State Electron 1987;30:953–68. http://dx.doi.org/10.1016/0038-1101(87)90132-8.
[56] García-Sánchez FJ, Ortiz-Conde A, De Mercato G, Liou JJ, Recht L, Eliminating parasitic resistances in parameter extraction of semiconductor device models. In: Proc First IEEE Int Caracas Conf on Devices, Circuits and Systems (ICCDCS); 1995. p. 298–302. http://dx.doi.org/10.1109/ICCDCS.1995.499164.
[57] García-Sánchez FJ, Ortiz-Conde A, Liou JJ. A parasitic series resistance-independent method for device-model parameter extraction. Proc Inst Elect Eng Circuit Dev Syst 1996;143:68–70. http://dx.doi.org/10.1049/ip-cds:19960159.
[58] Werner JH. Schottky barrier and pn-junction I/V plots – small signal evaluation. Appl Phys A: Solids Surf 1988;47(3):291–300. http://dx.doi.org/10.1007/BF00615935.
[59] Foty D, Binkley D, Bucher M. Starting over: Gm/Id-based MOSFET modeling as a basis for modernized analog design methodologies. In: International conference on modeling and simulation of microsystems – MSM; 2002. p. 682–5.
[60] Cunha AIA, Schneider MC, Galup-Montoro C, Caetano CDC, Machado MB. Unambiguous extraction of threshold voltage based on the transconductance-to-current ratio. WCM Nanotech 2005:139–41.
[61] Flandre D, Kilchytska V, Rudenko T. gm/Id method for threshold voltage extraction applicable in advanced MOSFETs with nonlinear behavior above threshold. IEEE Electron Dev Lett 2010;31:930–2. http://dx.doi.org/10.1109/LED.2010.2055829.
[62] Cunha AIA, Pavanello MA, Doria Trevisoli RD, Galup-Montoro C, Schneider MC. Direct determination of the threshold condition in DG-MOSFETs from the gm/ID curve. Solid-State Electron 2011;56:89–94. http://dx.doi.org/10.1016/j.sse.2010.10.011.
[63] Rudenko T, Kilchytska V, Arshad MKM, Raskin J-P, Nazarov A, Flandre D. On the MOSFET threshold voltage extraction by transconductance and transconductance-to-current ratio change methods: Part I-Effect of gate-voltage-dependent mobility. IEEE Trans Electron Dev 2011;58:4172–9. http://dx.doi.org/10.1109/TED.2011.2168226.
[64] Rudenko T, Kilchytska V, Arshad MKM, Raskin J-P, Nazarov A, Flandre D. On the MOSFET threshold voltage extraction by transconductance and transconductance-to-current ratio change methods: Part II-Effect of Drain Voltage. IEEE Trans Electron Dev 2011;58:4180–8. http://dx.doi.org/10.1109/TED.2011.2168227.
[65] Picos R, Garcia-Moreno E, Roca M, Iniguez B, Estrada M, Cerdeira A. Optimised design of an organic thin-film transistor amplifier using the gm/ID methodology. IET Circ Dev Syst 2012;6(2):136–40. http://dx.doi.org/10.1049/iet-cds.2011.0169.
[66] Rudenko T, Arshad MKMd, Raskin J-P, Nazarov A, Flandre D, Kilchytska V. On the gm/ID-based approaches for threshold voltage extraction in advanced MOSFETs and their application to ultra-thin body SOI MOSFETs. Solid-State Electron 2014;97:52–8. http://dx.doi.org/10.1016/j.sse.2014.04.029.
[67] Pollissard-Quatremere G, Gosset G, Flandre D. A modified gm/ID design methodology for deeply scaled CMOS technologies. Analog Integr Circ Sig Process 2014;78:771–84. http://dx.doi.org/10.1007/s10470-013-0166-z.
[68] Ghibaudo G. Critical MOSFETs operation for low voltage/low power IC's: ideal characteristics, parameter extraction, electrical noise and RTS fluctuations. Microelect Eng 1997;39(1–4):31–57. http://dx.doi.org/10.1016/S0167-9317(97)00166-4.
[69] Diouf C, Cros A, Monfray S, Mitard J, Rosa J, Gloria D, et al. "Y function" method applied to saturation regime: apparent saturation mobility and saturation velocity extraction. Solid-State Electron 2013;85:12–4. http://dx.doi.org/10.1016/j.sse.2013.03.007.
[70] Rahhal L, Bajolet A, Diouf C, Cros A, Rosa J, Planes N, et al. New methodology for drain current local variability characterization using Y function method. In: IEEE Int Conf Microelectronic Test Structures (ICMTS), 25–28 March 2013. p. 99–103. http://dx.doi.org/10.1109/ICMTS.2013.6528153.
[71] Mohd Razip Wee MF, Dehzangi A, Bollaert S, Wichmann N, Majlis BY. Gate length variation effect on performance of gate-first self-aligned $In_{0.53}Ga_{0.47}As$ MOSFET. PLoS ONE 2013;8(12):e82731. http://dx.doi.org/10.1371/journal.pone.0082731.
[72] Marinov O, Feng C, Deen MJ. Precise parameter extraction technique for organic thin-film transistors operating in the linear regime. In: 223rd ECS meeting of the electrochemical society; 2013. p. 824.
[73] Marinov O, Deen MJ, Feng C, Wu Y. Precise parameter extraction technique for organic thin-film transistors operating in the linear regime. J Appl Phys 2014;115:034506. http://dx.doi.org/10.1063/1.4862043.
[74] Fjeldly TA, Moon B-j, Shur M. Approximate analytical solution of generalized diode equation. IEEE Trans Electron Dev 1991;38(8):1976–7. http://dx.doi.org/10.1109/16.119046.
[75] Lee K, Shur M, Fjeldly TA, Ytterdal T. Semiconductor device modeling for VLSI. Prentice-Hall, Englewood Cliffs; 1993. <http://www.aimspice.com/>.